# Photoswitchable Molecular Units with Tunable Non-Linear Optical Activity: A Theoretical Investigation

Aggelos Avramopoulos * , Heribert Reis , Demeter Tzeli , Robert Zaleśny , Manthos Papadopoulos

Posted Date: 7 July 2023

doi: 10.20944/preprints202307.0483.v1

Keywords: (Hyper)polarizability; Density Functional Theory; Molecular Switches; Photochromism; Two-Photon absorption; Dithienylethene; bis(ethylene-1,2-dithiolato; Excited-state Energy Transfer

*Article*

# Photoswitchable Molecular Units with Tunable Non-Linear Optical Activity: A Theoretical Investigation

**Aggelos Avramopoulos [1,*], Heribert Reis [2], Demeter Tzeli [3,4], Robert Zalesny [5], and Manthos G. Papadopoulos [2]**

[1] Department of Physics, University of Thessaly, Lamia, 35100, Greece
[2] Institute of Chemical Biology, National Hellenic Research Foundation, Athens 11635, Greece
[3] Laboratory of Physical Chemistry, Department of Chemistry, National and Kapodistrian University of Athens, Athens, Greece
[4] Theoretical and Physical Chemistry Institute, National Hellenic Research Foundation, Athens 11635, Greece
[5] Faculty of Chemistry, Wrocław University of Science and Technology, Wyb. Wyspiańskiego 27, PL-50370 Wrocław, Poland
* aavramopoulos@uth.gr

**Abstract:** A series of derivatives, involving two dithienylethene (DTE), groups, connected by several molecular linkers (bis(ethylene-1,2-dithiolato)Ni- (NiBDT), naphthalene, quasilinear oligothiophene chains) are investigated with the aid of computational quantum chemistry methods. This involves the computation of the second- and third-order nonlinear optical properties, i.e. molecular hyperpolarizabilities of the designed/selected derivatives. These properties can be efficiently controlled by DTE switches, in connection with light of appropriate frequency. We found that NiBDT, as a linker, is associated with a greater contrast, in comparison to naphthalene, between the first and second hyperpolarizabilities of the "open-open" and the "closed-closed" isomers. This is explained by invoking the low lying excited states of NiBDT. It has been found that the second hyperpolarizability can be used as an index, which follows the structural changes induced by photochromism. The two-photon absorption, which is related to the imaginary part of second hyperpolarizability, has also been investigated for the $S_0 \rightarrow S_1$ transition. Furthermore, the intramolecular excited-state energy transfer (EET) is studied as well as the overlap between the absorption and emission spectra of the donor and acceptor groups of the molecules. The electronic coupling, $V_{DA}$, between the donor and acceptor fragments, as well as the emission spectrum of the donor and the absorption spectrum of the acceptor have been computed, assuming a Förster type transfer mechanism. EET is a critical factor governing the photochromism. Two methods were used to compute $V_{DA}$, one based on linear response and one based on the distributed multipole analysis (DMA); both techniques give very similar results for the dominating Coulomb contribution. For NiBDT as the linker a low $V_{DA}$ value has been computed. We found that $V_{DA}$ is affected by the molecular geometry. Our results clearly show that the linker strongly influences the communication between the open-closed DTE groups and thus, photochromism. The present computations show that full photochromism is attained in derivatives where two DTE groups are linked by a tetrathiophene chain, in agreement with experiment. The sensitivity of molecular linear and nonlinear optical properties upon photochromism can assist with the identification of the molecular isomers.

**Keywords:** (Hyper)polarizability; Density Functional Theory; Molecular Switches; Photochromism; Two-Photon absorption; Dithienylethene; bis(ethylene-1,2-dithiolato; Excited-state Energy Transfer

## Introduction

Multi-photochromic molecules are of current interest, since such systems allow to access up tp $2^n$ molecular states, if $n$ photochromic units are distinguishable, while molecules involving one photochromic unit are bistable [1,2]. For example, a derivative which involves two similar photochromic switches, may have the following states: "*open-open*" (**oo**), "*open-closed*" (**oc**), "*closed-*

Preprints (www.preprints.org) | NOT PEER-REVIEWED | Posted: 7 July 2023 doi:10.20944/preprints202307.0483.v1



*closed*" (**cc**). However, in several cases involving DTE switches, the "*closed-closed*" isomer is not observed. This has been attributed to Excitation Energy Transfer (EET) as an efficient competition process to the photoinduced cyclisation. The photo-activity of the involved photochromic groups depends on the linker or molecular bridge, which connects them.[2] It is understood that a saturated linker may allow the photochromic groups to retain their photo-activity.

EET is a process of great importance in many areas of research (e.g. biological systems, opto-electronic devices).[3] Of particular relevance to the present work, and the most frequent observed EET, is singlet excitation energy transfer (SEET). SEET has been used to rationalize several important processes (e.g. the light-harvesting in photosynthesis)[4]

An important parameter for the understanding of EET is the electronic coupling factor, between the two switching units; this is an off-diagonal Hamiltonian matrix element between the initial and final diabatic states in the transfer processes.[3] This coupling involves a Coulomb and a short-range term[3],[5] . At large separations the former reduces to the Förster dipole-dipole coupling.[5] The latter involves Dexter's exchange coupling[6] and an overlap term.[7] In solution, a further term related with the effect of the solvent may also be play a role[8] .

It has been established by early work that overlap of the donor fluorescence spectrum with the acceptor absorption spectrum ensures the energy conservation, in the weak coupling limit[9] . Kaieda et al[10]. studied the photocyclization of dithienylethene multimers and reported that the overlap of the fluorescence spectrum of the (**oo**) dimer and the absorption spectrum of the (**oc**) form, suggests that intramolecular energy transfer, from the excited open-ring fragment to the closed-ring unit, is possible.

*The effect of the bridge on the electronic coupling*

The significant role of the bridge on EET has been studied by several authors, in particular, Chen et al.[11] investigated the effect of the bridge on the Coulomb coupling, which makes the major contribution to the electronic coupling. They found that the EET rate increases, in comparison through-space models, when the donor and acceptor transition dipoles are arranged longitudinally and linked by a polarizable bridge (e.g. involving aromatic groups).

Scholes et al.[12] studied the through-space and through-bond effects on exciton interactions in a series of dinaphthyl molecules, in which the naphthyl units are connected by a polynorbornyl bridge. The enhancement of the energy delocalization by the through-bond interactions has been noted. Electronic coupling through rigid saturated spacers, involving up to 12 $\sigma$ bonds has been reported[12,13].

Energy transfer rates have been studied in donor-bridge-acceptor (D-B-A) systems[14]; several factors have been considered e.g. the bridge length[15,16], conformation[17], electronic properties[18]. McConnell's super-exchange theory for electron transfer[19] has also been frequently applied to energy transfer[14].

Kudernac et al.[20], in their study of uni- and bi-directional light-induced switching of DTEs, linked to the surface of gold nanoparticles, found that the ring-closure process, depends on the spacer.

If several DTE units are present in a molecule, a *stepwise* photo-cyclization process is significant. Non-conjugated linkers are associated with a fully ring-closed isomer,[21] because no SEET takes place. However, if $\pi$-conjugated linkers are involved, usually, a *partial* photochromism is observed, due to SEET.

*Computation of EET*

EET has been approximated by Förster's theory[9,22]. This approach has been successfully applied in many cases (e.g. in predicting EET rates)[22], however, there are several cases where it has failed)[23,24]. This method assumes that there is a very weak coupling between an open DTE unit (D) and a closed one (A) and that their spatial extensions are much smaller than $R_{DA}$ (the distance between D and A), so that the point-dipole approximation can be employed[22]. Several methods have been proposed for a more accurate description of EET[24,25] (e.g. transition monopole

 doi:10.20944/preprints202307.0483.v1



approximation[26] transition density cubes[27] and the fragment excitation difference (FED) method[3]).

Perhaps the simplest approach to calculate the electronic coupling between chromophores is to approximate it by the Coulomb interaction and to compute it by employing the transition dipole moments, that is, the point dipole approximation (PDA), which is an easy way to calculate the coupling, but it fails at short distances.[28] One may go beyond the dipole-dipole approximation to involve multipole couplings. For short distances these have been found to have significant contributions.[29] A less approximate approach to compute the Coulomb coupling is to use the density cube method.[27] The point dipole approximation (PDA) is frequently used, giving satisfactory results, when the distance between the donor and the acceptor ($R_{DA}$) is much larger than their dimensions. Overestimated results may be received at short distances. [30]

The study of molecular optical properties provides valuable information in several important areas (e.g. nano-structures).[31] Studies of single-molecules itself help us to probe and to understand mechanisms in a deeper detail and could be used to obtain information on what is happening at the nanoscale[31] The third-order nonlinear optical response of energy transfer systems has been studied theoretically by Young and Fleming. [32] The effect of molecular switching on the NLO properties has also been studied by several research groups. [33–35]. The stimuli (e.g. light irradiation, pH variation), which were used to induce the molecular transformation have also been discussed.[34] The DTE switches, in connection with light of appropriate frequency (which leads to "*open*" or "closed" DTE units) allow to control the molecular linear and nonlinear optical (L&NLO) properties efficiently, since the cyclization reaction increases the conjugation and thus polarization DTE multistate molecular materials have been considered as a research field of significant interest.[36] This is of great importance for several applications (e.g., data processing, photonic communication).[37] In addition, EET is a significant property of excited states and these states provide an important tool for the rationalization of the L&NLO properties. Thus, the photochromic properties of DTEs, their L&NLO and EET provide complementary information about the molecular structure.

Taking into account the aforementioned challenging issues, the following topics have been addressed here:

(i) The relationship between the molecular (hyper)polarizabilities of several derivatives consisting of 2 DTE units, with and without different substituents, and connected by different conjugated linkers, and the changes induced by photochromism on these properties. It is a major objective to find those structures and linkers, in particular, which lead to a significant contrast between the hyperpolarizabilities of the "*open*" and the "*closed*" isomers. A detailed discussion on the selection of the molecular linkers (molecular bridges ) used in this study is given in the Results and Discussion method.

(ii) The effect of the linker on the electronic communication of the DTE units and the photochromism as well as the intramolecular EET. A series of linkers has been selected in order to tune EET and eventually to minimize it, to attain full photochromism.

## II. Methods

We shall discuss the following topics in this section: (i) a definition of the hyperpolarizabilities, (ii) the functionals we have employed, (iii) the validation procedures we have used, (iv) the method used to compute the transition energies, (v) the computational approach employed to calculate the emission spectrum of the donor, the absorption spectrum of the acceptor and their overlap, (vi) the procedure used to compute two-photon absorption, (vii) the methods employed for the computation of the electronic coupling.

### *II.1. Definitions*

A Taylor series may be used for the expansion of the energy (E) of a molecule, which is placed in a static, uniform electric field ($F_i$) :[38]

Preprints (www.preprints.org) | NOT PEER-REVIEWED | Posted: 7 July 2023 doi:10.20944/preprints202307.0483.v1



$$E(F) = E^0 - \mu_i F_i - (1/2)\alpha_{ij}F_iF_j - (1/6)\beta_{ijk}F_iF_jF_k - (1/24)\gamma_{ijkl}F_iF_jF_kF_l - \ldots \quad (1)$$

where, $E^0$ is the field free energy and $\mu_i$ $\alpha_{ij}$ $\beta_{ijk}$ $\gamma_{ijkl}$, are the dipole moment, polarizability, first and second hyperpolarizability components, respectively; a summation over repeated indices is implied. The average (hyper)polarizabilities are defined by:

$$\alpha = \frac{1}{3}(\alpha_{xx} + \alpha_{yy} + \alpha_{zz}) \quad (2)$$

$$\beta = \sum_{i=x,y,z} \frac{\mu_i \beta_i}{\|\mu\|} \quad (3)$$

where $\beta_\iota$

$$\beta_i = \frac{1}{5}\sum_{j=x,y,z}(\beta_{ijj} + \beta_{jij} + \beta_{jji}) \quad (4)$$

$$\gamma = \frac{1}{5}(\gamma_{xxxx} + \gamma_{yyyy} + \gamma_{zzzz} + 2\gamma_{xxyy} + 2\gamma_{xxzz} + 2\gamma_{yyzz}) \quad (5)$$

The finite field perturbation theory (FPT) has been used for the calculation of the static (hyper)polarizabilities.[39] The Romberg-Rutishauer method[40–42] has been employed in order to safeguard the numerical stability of the computed (hyper)polarizability values. The computed static (hyper)polarizabilities values are expected to be useful for a relative comparison of the NLO properties of the studied photoswitchable compounds, since these are a good approximation to dynamic ones (frequency-dependent) in the off-resonant region.[43] The following field strengths have been used: $2^m$F, m=1-4 and F=0,0005 a.u.. The GAUSSIAN 16 software has been employed for the DFT computations (see below).[44]

*II.2. Functionals and Basis sets*

The following functionals have been used for the computation of the reported molecular properties:

**(i)** ***B3LYP***. This functional has been used to calculate the structure of the considered compounds. For all the molecular structures vibrational analysis was performed to verify that a real minimum has been found on the potential energy hyper-surface. B3LYP is a well-tested functional[45] which has been used for the determination of the structure of several other NiBDT derivatives.[46–49]. Its satisfactory performance has been also demonstrated in the literature.[50–52] For the case of the sexithiophene derivatives the conjugated skeleton is essentially planar, as shown experimentally in the crystal,[53] and this conformation is used in our computations. In order to further examine the performance of the B3LYP functional on the oligothiophene structures, we made geometry optimization of 1cc and 1oo molecules, R=Cl (Fig. 1)by employing the M062-X functional, since the latter has been shown to predict satisfactorily the geometries of π-conjugated systems, due to the appropriate amount (28%) of the included HF exchange. [54] The comparison between the geometries is shown in S.I material (Figure 1S).

**(ii)** ***CAM-B3LYP***. This long range corrected version of B3LYP[55] has been employed to compute the (hyper)polarizabilities of the considered derivatives. Detailed justification for its use has been reported in ref. [49]. The CAM-B3LYP functional[55] has also been used for the two-photon absorption calculations (II.6). We have employed the 6-31G* and cc-pVTZ basis set for H, C, O, F, and S atoms[56–59] and the quasi-relativistic effective core potential ECP28MWB(SDD) for the Ni atoms.[60] .

Preprints (www.preprints.org) | NOT PEER-REVIEWED | Posted: 7 July 2023 doi:10.20944/preprints202307.0483.v1



The adequacy of the CAM-B3LYP/6-31G* approach for the computation of the NiBDT properties is well documented.[46,48] NiBDT derivatives, having a singlet diradical character, should in principle be studied with a multiconfigurational wave function. However, it has been shown that broken-symmetry DFT [(U)DFT] gives satisfactoty property values.[46,49,61]

The electronic structure of the NiBDT derivatives, see Figure 5, have been studied via density functional theory (DFT) and time-dependent DFT (TD-DFT). The geometries of the structures are energetically optimized using the B3LYP[45] and the CAM-B3LYP[55] functionals and the 6-31G* basis set for H, C, O, F, and S atoms and the quasi-relativistic effective core potential ECP28MWB(SDD) for the Ni atoms.[52] The absorption and emission spectra of the studied structures were calculated via the TD-DFT. TD-DFT can predict absorption and emission spectra of molecules in very good agreement with experimental spectra.[62,63] Particularly, CAM-B3LYP functional has been developed to correct for the long-range behavior and it is regarded as appropriate for the computation of the absorption spectra when charge transfer states are involved. [64] Four main excited states were energetically optimized. In all cases, the absorption and emission spectra of the studied systems were calculated including up to 130 singlet-spin excited electronic states. All calculations were carried out with the Gaussian16 code. Time-dependent density functional theory (TD-DFT)[65,66] in connection with the CAM-B3LYP functional[55] has been used to compute the transition energies. It has been reported that this approach give satisfactory results.[67,68] All the reported computations were employed in the gas phase.

*II.3 Two-photon absorption*

The two-photon absorption (2PA) process is described by the imaginary part of the frequency-dependent second hyperpolarizability.[69–71] At the molecular scale, the two-photon absorption process is characterized by the second-order transition moment $S_{ab}$ that can be computed from the single residue of the quadratic response function.[72] In this work we assumed one source of photons and linearly polarized light. In such case, the orientationally averaged two-photon absorption strength for an isotropic medium can computed as :[73]

$$\langle\delta^{2PA}\rangle = \frac{1}{15}\sum_{ab}(S_{aa}\,S^{*}_{bb} + 2S_{ab}\,S^{*}_{ba}) \qquad (6)$$

$\langle\delta^{2PA}\rangle$, in what follows given in atomic units, is directly related to the two-photon absorption cross section ($\sigma^{2PA}$), which can be determined experimentally. The interested reader is referred to other work for conversion to macroscopic units (cross section is commonly expressed in Goppert-Mayer (GM) units).[74] The two-photon absorption calculations were performed using GAMESS US program [75,76] using CAM-B3LYP functional[55] and 6-31G(d) basis set. The choice of the CAM-B3LYP functional requires a proper justification. In the case of 2PA process, there are several striking reports regarding unsatisfactory performance of exchange–correlation functionals in predicting the magnitude of two-photon strengths.[55,74–77] For example, the CAM-B3LYP functional gives 2PA strengths that are often underestimated in comparison with the reference coupled-cluster values,[74] even though it improves upon conventional functionals in predicting excitation energies to charge-transfer states, as explained above. However, as recently demonstrated for a series of organic molecules, only range-separated functionals (CAM-B3LYP and LC-BLYP) correctly predict changes in $\delta^{2PA}$ upon chemical modifications and reproduce experimental trends. [78,79] The functionals with fixed amount of exact exchange fail to predict key parameters such as the transition moments between electronic states and excitation energies, such that their agreement with RI-CC2 reference data is due to error cancellations. Moreover, range-separated functionals such as CAM- B3LYP and LC-BLYP yield 2PA strengths which substantially deviate from reference values and this can be linked to underestimated excited-state dipole moments. However, the errors are rather systematic and these functionals nicely reproduce the chemical trends.

Preprints (www.preprints.org) | NOT PEER-REVIEWED | Posted: 7 July 2023 doi:10.20944/preprints202307.0483.v1



*II.4 Computation of the Electronic Coupling:*

The electronic coupling between the excitation of the donor (D) and the acceptor (A), $V_{DA}$, is of major importance for understanding EET; it appears in the energy transfer rate, $k_{EET}$,

$$k_{EET} = (2\pi/\hbar)\,|\,V_{DA}\,|^2 J, \qquad (7)$$

where J is the spectral overlap (i.e. the overlap integral) between the emission band of the donor and the absorption band of the acceptor.[1] We have computed $V_{DA}$ by two methods: one based on the linear response method and the other based the distributed multipole approach.

*Linear response method*. According to this approach $V_{DA}$ is given by:[80]

$$V_{DA} = \int d\mathbf{r} \int d\mathbf{r}' \rho_D^{tr*}(r) \frac{1}{|r-r'|} \rho_A^{tr}(r') + \int d\mathbf{r} \int d\mathbf{r}' \rho_D^{tr*}(r) g_{xc}(r,r') \rho_A^{tr}(r') - \omega_0 \int d\mathbf{r} \rho_D^{tr}(r) \rho_A^{tr}(r) \qquad (8)$$

$\varrho^{tr}$ gives the transition density of the donor and the acceptor. The Coulomb interaction between the transition densities is given by the first term, $g_{xc}$ is the exchange-correlation kernel, and the second term gives the exchange-correlation interaction; $\omega_0$ is the average resonance transition energy of the dimer, while the third term gives a correction contribution.

***Distributed multipole analysis***. For very large molecules the computational cost of the analytical calculation of the EET terms may be prohibitively large and a more economic method would be useful. For the Coulomb term, which is generally the largest contribution to the EET coupling, several schemes based on a more sophisticated treatment of the transition densities have been published (see, e.g. the literature cited in Ref. [81] to overcome the shortcomings of the original point dipole treatment using molecular transition dipole moments by Förster.[82] A particularly accurate and computationally economical method, based on the distributed multipole expansion of the transition densities, has been published by Błasiak et al.[81] In this approach, the electrostatic part of the EET coupling between two excited molecules is computed using transition-density derived cumulative atomic multipole moments (TrCAMM). We have here applied a similar method, replacing TrCAMM by the distributed multipole analysis (DMA), pioneered by Stone.[83,84] Apart from this change, the approach was used as described in Ref. [81], to which we refer for further details. The transition densities required where computed using Multiwfn 3.7 ,[85] and the distributed multipole analysis was performed with the GDMA 2.3.3 program. [86] Preliminary tests using several ethylene and naphthalene dimers in the same configuration as used in Ref. [81] have been performed to ensure that the substitution of TrCAMM by DMA still leads to viable results; the differences to the values reported in Ref. [81] were smaller than 5%.

## III. Results and Discussion

In this section we shall consider: (i) the static (hyper)polarizabilities of 2 DTE units with and without different substituents and connected by a quasilinear tetrathiophene chain as well as 2 DTE units connected by NiBDT and naphthalene as linkers, (ii) the two-photon absorption of selected thiophenes and (iii) the excited energy transfer (EET).

As mentioned in the introduction, the linker is of crucial importance for the communication between the open-closed DTE units and for the modulation of the molecular NLO properties. Three types of molecular bridges were selected: (a) a quasilinear tetrathiophene chain (see Fig. 1), which is known for its remarkable electronic and optoelectronic properties[53] (b) NiBDT which provides an excellent basis for the formation of molecular materials with exceptional optical, electronic and conductive properties[87] and finally naphthalene, which involves two fused benzene rings; this is a 10π electron system similar to NiBDT. It is also noted that two derivatives of molecule **1** (Fig. 1) with R=Cl and R=Phenyl, have been synthesized and their photochromism studied , thus allowing to compare the predicted ring closure of both DTE groups with the corresponding experimental finding. A 1D π-conjugated NiBDT nanosheet has also been synthesized.[88]

The main reasons for selecting the above bridges are, first, the expected significant contrast in the NLO properties of the three isomers (**oo**, **oc** and **cc**) and second, the interesting and challenging properties associated with the low-lying excited states of NiBDT, in connection with EET. It is also

Preprints (www.preprints.org) | NOT PEER-REVIEWED | Posted: 7 July 2023 doi:10.20944/preprints202307.0483.v1



noted that each molecular structure (**cc,co,cc**) is studied separately, in its lowest energy conformation, since we are interested in probing and understanding the relationship EET-NLO activity mechanism in more detail. Eventually, we want to understand how to attain full photochromism by modifying the molecular structure.

*III.1 (Hyper)polarizabilities*

The photochemical process leads to a large change of the structure, which is accompanied by very structure sensitive first and second hyperpolarizability properties (Tables 1 and 2).

**Table 1.** The (hyper)polarizabilities of the 1cc, 1oc and 1oo (Figure 1). The structures have been computed with the B3LYP/6-31G* method and the (hyper)polarizabilities with the CAM-B3LYP/6-31G*. All values are given in a.u.

| | α | | | β | | | γ (x10³) | | |
|---|---|---|---|---|---|---|---|---|---|
| **R** | **1cc** | **1co** | **1oo** | **1cc** | **1co** | **1oo** | **1cc** | **1co** | **1oo** |
| **H** | 972.6<br>1049.5[3] | 882.3 | 796.9 | 680<br>790[3] | 14860 | 150 | 14111<br>14660[3] | 8476 | 4078 |
| **Cl** | 1025.4<br>1108.0[3] | 926.0 | 827.2 | 1200<br>1250[3] | 20860 | 243 | 15635<br>16270[3] | 9299 | 4185 |
| | 914.0[4] | 824.6[4] | 776.7[4] | 1960[4] | 11700[4] | 144[4] | 8654[4] | 4719[4] | 2837[4] |
| **$NO_2$** | 1123.8 | 988.8 | 842.5 | 257 | 48040 | 773 | 22841 | 13260 | 4284 |
| **$NH_2$** | 1024.4 | 918.9 | 822.2 | 530 | 401 | 486 | 16212 | 8949 | 4208 |
| **Ph** | 1239.1 | 1096.1 | 960.8 | -310 | 10140 | 150 | 23611 | 12378 | 4692 |
| **$NO_2/NH_2$[1]** | 1094 | 930.0 | 832.4 | 71350 | 2950 | 4950 | 25370 | 9049 | 4272 |
| **$NO_2/NH_2$[2]** | | 988.0 | | | 61260 | | | 14861 | |

[1] NO2/NH2 groups are anchored on open/closed unit. [2] NO2/NH2 groups are anchored on closed/open unit. [3] Basis Set: C,S,F,Cl,H: cc-pVTZ, [4] Properties have been computed at the M062-X optimized geometry.

**Table 2.** The absorption wavelength (λ;nm) of the lowest lying allowed transition and the (hyper)polarizabilities (a.u.) of 2oo, 2oc, 2cc, 3oo and 3cc (Figure 2).

| **Derivative** | **λ** | **α** | **β** | **γ(x10³)** |
|---|---|---|---|---|
| **2oo** | 622.3[1] | 880.3[1] | -410[1] | 2741[1] |
| **2oc** | 884.1[1] | 1163[1] | 1349[1] | 17400[1] |
| | | 1225[2] | 1330[2] | 19236[2] |
| **2cc** | 994.3[1] | 1576.9[1] | -14076[1] | 67870[1] |
| | | 1652.5[2] | -13080[2] | 68890[2] |
| **3oo** | 614.0[1] | 792.9[1] | 432[1] | 1416[1] |
| **3cc** | 878.9[1] | 1129.6[1] | 5800[1] | 13971[1] |

1 (U) CAMB3LYP/6-31G*. [32] Basis Set: C,S,F,H: cc-pVTZ, Ni: SDD.

Preprints (www.preprints.org) | NOT PEER-REVIEWED | Posted: 7 July 2023 doi:10.20944/preprints202307.0483.v1



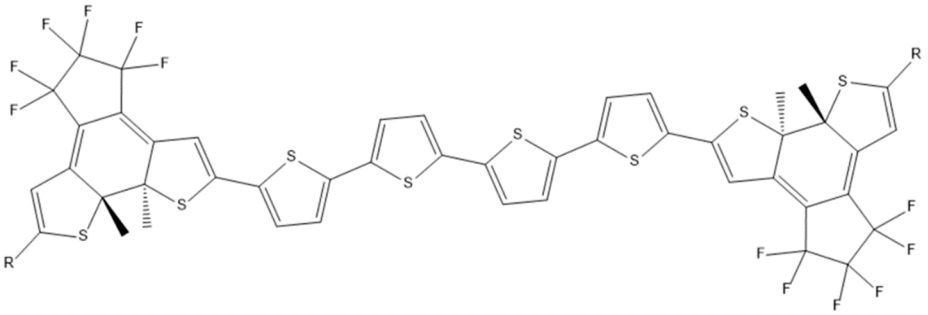

**1cc**

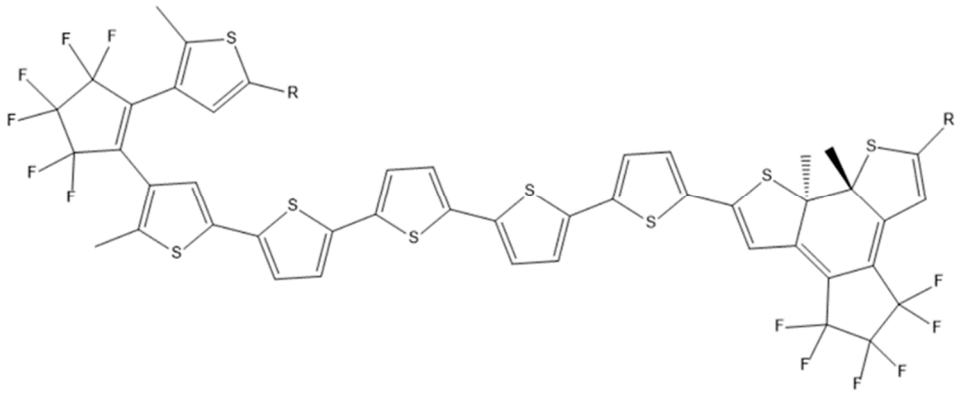

**1oc**

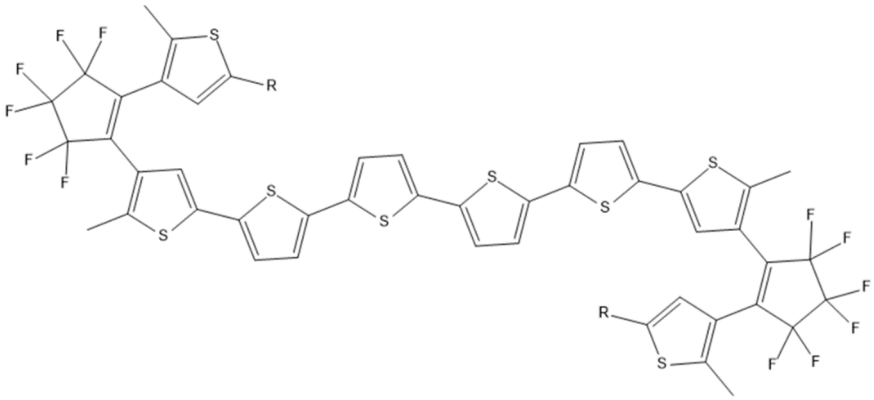

**1oo**

**Figure 1.** The structures of 1**cc**, 1**co** and 1**oo** computed with the B3LYP/6-31G* method.

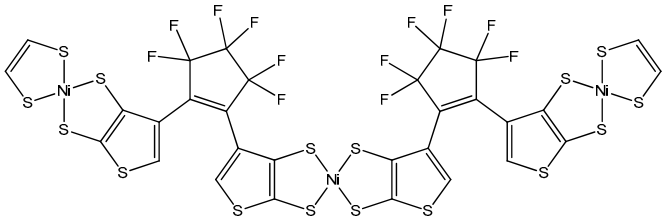

**2oo**

Preprints (www.preprints.org) | NOT PEER-REVIEWED | Posted: 7 July 2023 doi:10.20944/preprints202307.0483.v1



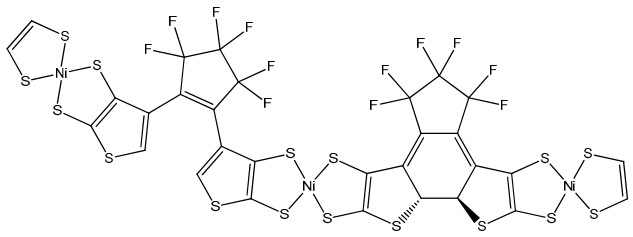

**2oc**

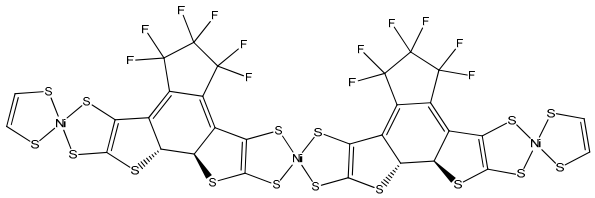

**2cc**

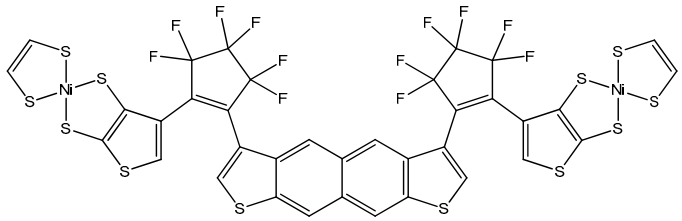

**3oo**

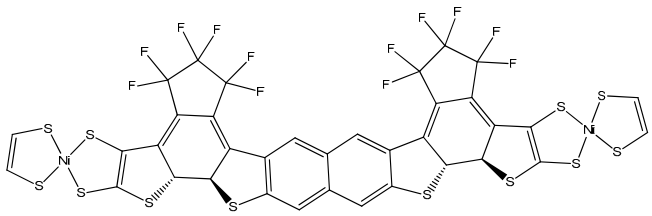

**3cc**

**Figure 2.** The structures of 2**oo**, 2**oc**, 2**cc,** 3**oo** and 3**oc**, computed with the B3LYP/6-31G* method.

A. Oligothiophenes

A series of derivatives with two DTE groups connected by a tetrathiophene group have been studied (Table 1; Figure 1), with different substituents R/R: H/H, Cl/Cl, $NO_2/NO_2$, $NH_2/NH_2$, Ph/Ph and $NO_2/NH_2$ on the DTE groups. We note that these derivatives may also be considered as alkene, methyl end-capped sexithiophenes, which may be a more adequate characterization at least for the open-open isomers.[87]

***Polarizabilities.*** The average polarizabilities of the "open-open" (oo) isomers are: 879±82 a.u. (Table 1), where the limits denote the maximum and minimum average polarizability values among the oo isomers. For the "open-closed" (oc) and "closed-closed" (cc) isomers the corresponding values are 989±107 a.u. and 1106±133 a.u., respectively. The observed trend is $\alpha$(**cc**)> $\alpha$(**oc**)> $\alpha$(**oo**); this is explained by the increased conjugation associated with the closed DTE thus increasing the electron mobility. For R=Ph, as expected, we observe the larger polarizability.

***First hyperpolarizabilities***. The largest β value is observed for the pair ,R: $NO_2/NH_2$ of **1cc** (71350 a.u.) and **1co** (61250 a.u.) isomers (Figure 1). This pair of substituents gives very different first hyperpolarizability values depending heavily on the state of the DTE unit (closed or open) to which they are bonded. For the **1co** isomer the larger β value is observed when $NO_2$ is bonded to the closed DTE unit and $NH_2$ is bonded to the open one. The tetrathiophene unit is conjugated (Figure 1). We shall now consider the effect of the extension of the conjugation path due to the closed DTE unit(s).

Preprints (www.preprints.org) | NOT PEER-REVIEWED | Posted: 7 July 2023 doi:10.20944/preprints202307.0483.v1



The effect of extending the conjugation path on β may be seen when R: H/H (Table 1); the maximum β value (14860 a.u.) is observed for **1co**.

The impact of *extending the conjugation path* on the first hyperpolarizability may also be seen when R: Cl/Cl, $NO_2/NO_2$. $NH_2/NH_2$ or Ph/Ph, but in these cases *charge-transfer* may also affect the results. The effect of *charge-transfer* on β, may be seen by the difference:

$$\Delta 1 = \beta(\text{Is; R:NO}_2/\text{NH}_2) - (\beta(\text{Is; R:NO}_2/\text{NH}_2) + \beta(\text{Is; R:NH}_2/\text{NO}_2))/2, \quad (9)$$

where, Is: **1cc**, **1oc** or **1oo**.

This difference takes the values 70956 a.u., [-21270], 37040 a.u., and 4321 a.u. for **1cc**, [1co], **1oc** or **1oo**, respectively (Table 1). The effect of charge-transfer, as a function of conjugation, upon photoswitching, may be expressed by the above sequence of values. We observe that the molecular state, the conjugation and the charge transfer have a very significant effect on the first hyperpolarizability (β).

***Second hyperpolarizabilities***. Larger property values are observed for the cc isomer, as it would be expected due to the conjugation; the following trend is observed: γ(**cc**)> γ(**oc**)> γ(**oo**) (Table 1). In particular we note, the effect of *extending the conjugation path* on γ may be seen by comparison with R,R':H/H; the maximum second hyperpolarizability value is observed for **1cc** (14111x$10^3$ a.u.). The effect of *charge-transfer* on γ, may be estimated by the difference:

$$\Delta 2 = \gamma(\text{Is; R,R':NO2/NH2}) - (\gamma(\text{Is; R,R':NH2/NO2}) + \gamma(\text{Is; R,R':NO2/NH2}))/2, \quad (10)$$

where, Is: **1cc, 1co, [1oc]** or **1oo**. This difference takes the values 5844 x$10^3$ a.u., [-2056], 3757 x$10^3$ a.u., and 26 x$10^3$ a.u. for **1cc**, [1co], **1oc** and **1oo**, respectively (Table 1*)*. Again, the effect of charge-transfer, as a function of the conjugation length may be expressed by the above sequence of values. We observe that both conjugation enhancement, upon photoswithing, and charge transfer have a very significant effect on the second hyperpolarizability (γ).

Taking the ratios Δ1(**1cc**)/Δ1(**1oo**) = 16.9 ( (eq. 9) and Δ2(**1cc**)/Δ2(**1oo**) = 224.8 (eq. 10), we observe that the effect of *charge-transfer*, as a function of *conjugation* has a much greater effect on γ than on β. The corresponding ratio for the polarizability (α) is 3.4. In general α obeys most of the trends of γ, but in a less pronounced way. Finally let us also note that for the case of α and γ, change of the geometry (B3LYP/M062-X) has s small effect on the contrast ratios, k=$P_{1cc}/P_{1oo}$ and λ= $P_{1cc}/P_{1co}$ (Table 1;R=Cl). It is observed that k=1,24/1.17(α), 3.74/3.05 (γ) , while λ=1.11/1.11 (α), 1,68/1.83(γ). The notation A/B(P) stands for the ratio computed at the B3LYP/M062-X optimized geometry and P=α,γ denotes the property. For the case of β the effect was found to be larger and stands for k=4.9/13.6 and λ=0.06/0.17.

B. Derivatives Having NiBDT and Naphthalene as Linkers

A series of derivatives have been studied, which involve two DTE groups, connected by either NiBDT or naphthalene (Figure 2; Table 2). Both linkers have 10π electrons.

***NiBDT.*** We observe that the cc isomer lies lower in total energy compared with **oc** and **oo** ones (Table 1S):

E(**2oo**)> E(**2oc**)> E(**2cc**),

We also observe that an increase of conjugation, upon photoswitching, leads to a decrease of the |HOMO-LUMO| (=$\Delta_{HL}$) gap (Table 1S), due to destabilization of HOMO; for **2oo**, **2oc** and **2cc** the corresponding $\Delta_{HL}$ values are 0.059 a.u., 0.050 a.u. and 0.042 a.u., respectively. Let us note that a similar trend was found for the sexithiophene derivatives (Table 1S)

These results are in agreement with those reported in the literature.[89] A red-shift of $\lambda_{max}$ is also noted, upon changing the structure of the isomer: λ(**2cc**)> λ(**2oc**) λ(**2oo**) (Table 2).

For the (hyper)polarizabilities we observe the trend (Table 2): P(**2cc**)> P(**2oc**)> P(**2oo**), where P: α, |β|, γ. The cc isomer has remarkably larger properties (α, |β|, γ) values than the other isomers.

***Naphthalene.*** For the total energy we also observe that: E(**3oo**)> E(**3cc**) (Table 2). A similar trend was found for NiBDT as a linker. For the (hyper) polarizabilities, we found: P(**cc**)> P(**oo**), P=α,β,γ. A significant change for β and γ of **oo** and **cc** isomers is also observed.

NiBDT and Naphthalene have both 10π electrons, however their effect on α, β, and γ is very different. For NiBDT, as a bridge, the ratio of $P_{2cc}/P_{2oo}$, where P= α, β, or γ is 1.8, 34.3 and 24.7,

Preprints (www.preprints.org) | NOT PEER-REVIEWED | Posted: 7 July 2023 doi:10.20944/preprints202307.0483.v1



respectively, while for napthalene the corresponding ratios for **3cc**/**3oo** are 1.42($\alpha$), 13.4($\beta$) and 9.9($\gamma$). The ratio $P_{2cc}/P_{3cc}$, which shows the effect of the type of the bridge on the L&NLO molecular properties is 1.4, -2.4 and 4.9 for $\alpha$, $\beta$, and $\gamma$, respectively. As it has been shown, the existence of low lying excited states, due to the presence of NiBDT, significantly enhances the polarization character.[90]

In the previous article [49] we have investigated the contrast between the L&NLO properties of the "open" and "closed" isomer of the derivatives involving one DTE unit. [49] We found that P(**c**)>P(**o**), where P: $\alpha$ or $\gamma$. In this work, the considered molecules involve two DTE groups. We observe, in general, P(**cc**)>P(**co**)>P(**oo**), where P: $\alpha$ or $\gamma$. This trend is due to an increase of conjugation, upon photoswitching, in the order **cc**>**oc**>**oo**. As shown in Ref [49] increasing the conjugation path increases the positive contribution of the density of the second hyperpolarizability much more than the negative one, thus reinforcing the $\gamma$ values. The trends observed in the first hyperpolarizability are less regular.

Summarizing the findings from Tables 1&2, we note that the molecular L&NLO optical properties follow the structural changes induced by photochromism. The first hyperpolarizability ($\beta$) shows a less regular dependence in comparison to polarizability ($\alpha$) and second hyperpolarizability ($\gamma$). There is a significant contrast between the computed values, for the first and second hyperpolarizabilities of the open-open and closed-closed isomers of the considered derivatives. NiBDT as a linker leads to a greater contrast, in comparison to naphthalene and oligothiophene. The great effect of conjugation on the hyperpolarizabilities is clearly demonstrated by the closed-closed isomers. The results (Tables 1 & 2) show that the hyperpolarizabilities and in particular $\gamma$ can be used as an index, which follows the structural changes induced by photochromism. Therefore, the sensitivity of the polarization character upon photoswitching can assist to the identification of the molecular isomers (**oo-oc-cc**) upon light irradiation. To reinforce the validity of the basis set 6-31G* for the properties considered here, we have computed selected cases with the larger basis set cc-pVTZ. As shown in Tables 1,2 there is a reasonable agreement between the two sets of data.

***HOMA analysis.*** To obtain a further insight into the reasons for the differences of the hyperpolarizabilities for the different isomers, we computed a measure for the conjugation along the quasilinear conjugated $[\text{-C=C-}]_n$ chain, following the prescription of the Harmonic Oscillator Model of Aromaticity (HOMA) index $I_{HOMA}$ [91]:

$$I_{HOMA} = 1 - \frac{\alpha}{n}\sum_{i=1}^{n}(R_i - R_{Opt})^2 \ , \qquad (11)$$

where $n$ is the number of CC bonds, $R_i$ is the $i$-th bond length of the conjugated chain, $R_{Opt}$ is the reference bond length in benzene, chosen as an optimally conjugated system and computed at the same level of theory (1.397 Å at B3LYP/6-31G*), and 257.7 $Å^{-2}$ is a normalization factor chosen such that $I_{HOMA}$ of an aromatic compound approaches 1 and that of its Kekulé non-aromatic structure becomes 0.

The HOMA index was computed for two of the $R_1$-1xy-$R_2$ series of isomers (x,y=c,o); a) with $R_1$=$NO_2$, $R_2$=$NH_2$, and b) with $R_1$=$R_2$=H. For the internal $[\text{-C=C-}]_{21}$ chain, which can be written as a neutral, fully conjugated pseudolinear structure in all isomers, the calculated HOMA indices using eq. 11, with n=21, are shown in Table 3. For both molecules the conjugation as measured by the HOMA index increases with the number of closed ring structures.

**Table 3.** Computed HOMA index of $NO_2$-1AB-$NH_2$ and H-1AB-H, A,B = c,o.

| | **1cc** | | | **1oc** | | | **1oo** | | |
|---|---|---|---|---|---|---|---|---|---|
| | **ΔE** | **f** | **$\langle\delta^{2PA}\rangle$ ×10³** | **ΔE** | **f** | **$\langle\delta^{2PA}\rangle$ ×10³** | **ΔE** | **f** | **$\langle\delta^{2PA}\rangle$ ×10³** |
| $S_0 \rightarrow S_1$ | 2.162 | 2.3537 | <0.1 | 2.243 | 1.4665 | 7.0 | 2.820 | 2.5150 | <0.1 |
| $S_0 \rightarrow S_2$ | 2.344 | 0.0159 | 0.2 | 2.843 | 1.2518 | 113.3 | 3.543 | 0.0226 | 8.6 |
| $S_0 \rightarrow S_3$ | 2.885 | 0.6755 | 0.4 | 3.436 | 0.0660 | 1512.2 | 3.994 | 0.0236 | <0.1 |
| $S_0 \rightarrow S_4$ | 3.340 | 0.0008 | 6690.7 | 3.648 | 0.0164 | 2358.2 | 4.023 | 0.0380 | 126.0 |
| $S_0 \rightarrow S_5$ | 3.577 | 0.0002 | 3105.5 | 3.793 | 0.0868 | 19.5 | 4.156 | 0.0030 | 2023.3 |

Preprints (www.preprints.org) | NOT PEER-REVIEWED | Posted: 7 July 2023 doi:10.20944/preprints202307.0483.v1



*III.2 Two-photon Absorption*

The electronic structure parameters (excitation energies, oscillator strengths and two-photon transition strengths) corresponding to five lowest-energy electronic excitations of **1cc,1co,1oo** molecules(Fig. 1, R=H) are shown in Tables 4–9. Note that the values of two-photon absorption (2PA) strengths for higher lying states ($S_4$-$S_5$) are not very accurate due to resonance effects (they are overestimated). In order to obtain more realistic values on should employ damped response theory,[92] but given the size of the studied systems such calculations were not feasible. We will start with the analysis of one-photon absorption properties. The data shown in Tables 4–9 allow to draw a few general comments.

**Table 4.** Excitation energy (ΔE, [eV]), oscillator strength (f) and two-photon transition strength ($\langle\delta^{2PA}\rangle$, [au]) corresponding to five lowest-energy electronic transitions for molecule R=Cl (Figure 1).

| | **$NO_2$-1AB-$NH_2$** | | | | **H-1AB-H** | | |
|---|---|---|---|---|---|---|---|
| AB | **cc** | **co** | **oc** | **oo** | **cc** | **oc** | **oo** |
| $I_{HOMA}$ | 0.827 | 0.806 | 0.807 | 0.778 | 0.843 | 0.812 | 0.790 |

**Table 5.** Excitation energy (ΔE, [eV]), oscillator strength (f) and two-photon transition strength ($\langle\delta^{2PA}\rangle$, [au]) corresponding to five lowest-energy electronic transitions for molecule R=H (Figure 1).

| | **1cc** | | | **1oc** | | | **1oo** | | |
|---|---|---|---|---|---|---|---|---|---|
| | ΔE | f | $\langle\delta^{2PA}\rangle$ ×$10^3$ | ΔE | f | $\langle\delta^{2PA}\rangle$ ×$10^3$ | ΔE | f | $\langle\delta^{2PA}\rangle$ ×$10^3$ |
| $S_0\rightarrow S_1$ | 2.169 | 2.1698 | <0.1 | 2.252 | 1.3319 | 3.2 | 2.819 | 2.4780 | <0.1 |
| $S_0\rightarrow S_2$ | 2.344 | 0.0114 | 1.8 | 2.844 | 1.3222 | 94.1 | 3.544 | 0.0208 | 5.2 |
| $S_0\rightarrow S_3$ | 2.878 | 0.7472 | 0.3 | 3.450 | 0.0534 | 1192.0 | 4.045 | 0.0252 | <0.1 |
| $S_0\rightarrow S_4$ | 3.353 | 0.0002 | 5802.2 | 3.643 | 0.0144 | 2168.1 | 4.080 | 0.0337 | 431.2 |
| $S_0\rightarrow S_5$ | 3.556 | 0.0002 | 2516.0 | 3.748 | 0.0822 | 25.3 | 4.162 | 0.0106 | 1657.9 |

**Table 6.** Excitation energy (ΔE, [eV]), oscillator strength (f) and two-photon transition strength ($\langle\delta^{2PA}\rangle$, [au]) corresponding to five lowest-energy electronic transitions for molecule R=$NH_2$ (Figure 1).

| | **1cc** | | | **1oc** | | | **1oo** | | |
|---|---|---|---|---|---|---|---|---|---|
| | ΔE | f | $\langle\delta^{2PA}\rangle$ ×$10^3$ | ΔE | f | $\langle\delta^{2PA}\rangle$ ×$10^3$ | ΔE | f | $\langle\delta^{2PA}\rangle$ ×$10^3$ |
| $S_0\rightarrow S_1$ | 2.161 | 2.4581 | <0.1 | 2.253 | 1.5232 | 2.8 | 2.817 | 2.5106 | <0.1 |
| $S_0\rightarrow S_2$ | 2.353 | 0.0150 | 31.9 | 2.885 | 1.2299 | 41.8 | 3.540 | 0.0226 | 2.6 |
| $S_0\rightarrow S_3$ | 2.935 | 0.5549 | 0.3 | 3.526 | 0.0218 | 1966.6 | 3.940 | 0.0263 | 1.0 |
| $S_0\rightarrow S_4$ | 3.382 | 0.0005 | 9561.7 | 3.562 | 0.0402 | 1807.8 | 3.949 | 0.0974 | 13.5 |
| $S_0\rightarrow S_5$ | 3.544 | 0.0002 | 1.6 | 3.905 | 0.0294 | 25.9 | 4.128 | 0.0018 | 1927.5 |

**Table 7.** Excitation energy (ΔE, [eV]), oscillator strength (f) and two-photon transition strength ($\langle\delta^{2PA}\rangle$, [au]) corresponding to five lowest-energy electronic transitions for molecule R=$NO_2$ (Figure 1).

| | **1cc** | | | **1oc** | | | **1oo** | | |
|---|---|---|---|---|---|---|---|---|---|
| | ΔE | f | $\langle\delta^{2PA}\rangle$ ×$10^3$ | ΔE | f | $\langle\delta^{2PA}\rangle$ ×$10^3$ | ΔE | f | $\langle\delta^{2PA}\rangle$ ×$10^3$ |
| $S_0\rightarrow S_1$ | 1.932 | 2.0938 | <0.1 | 1.984 | 1.1765 | 49.1 | 2.820 | 2.5449 | <0.1 |
| $S_0\rightarrow S_2$ | 2.068 | 0.0024 | 39.1 | 2.691 | 1.4493 | 367.0 | 3.539 | 0.0248 | 20.3 |
| $S_0\rightarrow S_3$ | 2.696 | 1.0551 | <0.1 | 3.229 | 0.1597 | 3058.4 | 3.840 | 0.0130 | 0.4 |
| $S_0\rightarrow S_4$ | 3.089 | 0.0009 | 10167.0 | 3.374 | 0.1308 | 715.1 | 3.853 | 0.0056 | 20.2 |

Preprints (www.preprints.org) | NOT PEER-REVIEWED | Posted: 7 July 2023 doi:10.20944/preprints202307.0483.v1



| | | | | | | | | | |
|---|---|---|---|---|---|---|---|---|---|
| $S_0 \rightarrow S_5$ | 3.322 | 0.0006 | 4760.5 | 3.468 | 0.0753 | 9.2 | 3.912 | 0.0003 | <0.1 |

**Table 8.** Excitation energy (ΔE, [eV]), oscillator strength (f) and two-photon transition strength ($\langle\delta^{2PA}\rangle$, [au]) corresponding to five lowest-energy electronic transitions for molecule R=$NO_2$, R'=$NH_2$ (Figure 1).

| | **1cc** | | | **1oc**[a)] | | | **1oo** | | |
|---|---|---|---|---|---|---|---|---|---|
| | ΔE | f | $\langle\delta^{2PA}\rangle$ ×$10^3$ | ΔE | f | $\langle\delta^{2PA}\rangle$ ×$10^3$ | ΔE | f | $\langle\delta^{2PA}\rangle$ ×$10^3$ |
| $S_0 \rightarrow S_1$ | 1.951 | 1.7422 | 118.4 | 2.249 | 1.5157 | 8.3 | 2.817 | 2.5218 | 3.5 |
| $S_0 \rightarrow S_2$ | 2.243 | 0.6864 | 85.5 | 2.886 | 1.2587 | 9.6 | 3.538 | 0.0245 | 9.3 |
| $S_0 \rightarrow S_3$ | 2.704 | 0.3358 | 1286.2 | 3.528 | 0.0035 | 3251.3 | 3.799 | 0.0068 | 9.3 |
| $S_0 \rightarrow S_4$ | 3.002 | 0.3582 | 2916.7 | 3.542 | 0.0658 | 557.8 | 3.912 | 0.0002 | 0.2 |
| $S_0 \rightarrow S_5$ | 3.253 | 0.0042 | 1586.6 | 3.777 | 0.0015 | 0.6 | 3.951 | 0.0583 | 5.3 |

[a] $NO_2$ group attached to "open" moiety.

**Table 9.** Excitation energy (ΔE, [eV]), oscillator strength (f) and two-photon transition strength ($\langle\delta^{2PA}\rangle$, [au]) corresponding to five lowest-energy electronic transitions for molecule R=$NO_2$, R'=$NH_2$. (Figure 1).

| | **1oc**[a] | | |
|---|---|---|---|
| | ΔE | f | $\langle\delta^{2PA}\rangle$ ×$10^3$ |
| $S_0 \rightarrow S_1$ | 1.972 | 1.2258 | 70.5 |
| $S_0 \rightarrow S_2$ | 2.650 | 1.3286 | 541.5 |
| $S_0 \rightarrow S_3$ | 3.195 | 0.2143 | 3036.5 |
| $S_0 \rightarrow S_4$ | 3.360 | 0.1164 | 743.6 |
| $S_0 \rightarrow S_5$ | 3.460 | 0.0732 | 11.5 |

[a] $NO_2$ group attached to "closed" moiety.

First, for all considered substituents, the $S_0 \rightarrow S_1$ transition is characterized by very large values of oscillator strengths (spanning the range 1.18 (R=$NO_2$, **oc**) – 2.54 (R=$NO_2$, **oo**)).

Second, there is a common pattern for all compounds for this transition:

ΔE(**cc**) < ΔE(**oc**) < ΔE(**oo**) and

f(**oc**) < f(**cc**) < f(**oo**)

Third, for **cc** and **oc** isomers with R=$NO_2$ and R=$NO_2$, $NH_2$ substituents there is a moderate change in $S_0 \rightarrow S_1$ excitation energy in comparison to other derivatives (R=Cl, R=H, R=$NH_2$). However, for **oo** we note that the $S_0 \rightarrow S_1$ excitation energy is insensitive to the change of substituent, i.e. it is roughly 2.8 eV. The 2PA properties corresponding to the $S_0 \rightarrow S_1$ transition are negligible (i.e. less than $10^4$ au) for most of the compounds. There are only three exceptions, i.e. **oc** isomer (R=$NO_2$; Table 7)), **cc** and **oc** with R=$NO_2$, R'=$NH_2$ (Tables 8 and 9). The corresponding values for all three cases exceed $5\times10^4$ and reach up to $12\times10^4$ (**cc** isomer). Taken together, these results demonstrate that in the case of bright $S_0 \rightarrow S_1$ transition it is possible to tune the excitation energies and 2PA transition strengths by changing substituents only for cc and **oc** isomers. The most pronounced change in properties is achieved by using asymmetric substitution by $NO_2$ and $NH_2$ and 2PA strengths can be increased by two orders of magnitude.

*III. 3 Excitation Energy Transfer*

The intra-molecular EET and the overlap between absorption and emission spectra of the studied systems will be analyzed. The intra-molecular process depends on a number of factors (e.g. $V_{DA}$ – the electronic coupling between the donor and the acceptor-, the overlap of the emission spectrum of the donor and the absorption spectrum of the acceptor). By necessity this study has to be

Preprints (www.preprints.org) | NOT PEER-REVIEWED | Posted: 7 July 2023 doi:10.20944/preprints202307.0483.v1



selective. Thus, analysis of the intra-molecular EET will rely on $V_{DA}$. Additionally, the overlap of the emission spectrum of the donor and the absorption spectrum of the acceptor will be studied.

The selected bridges, between the DTE units (Figures 1–3), allow to tune $V_{DA}$ and eventually EET. In this context, it is useful to find out how the modification of structure affects $V_{DA}$. In particular, it is important to specify rules to minimize EET and thus to attain full photochromism. This is a central question of our study.

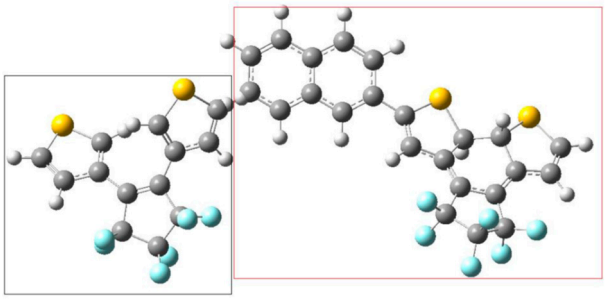

**4oc**

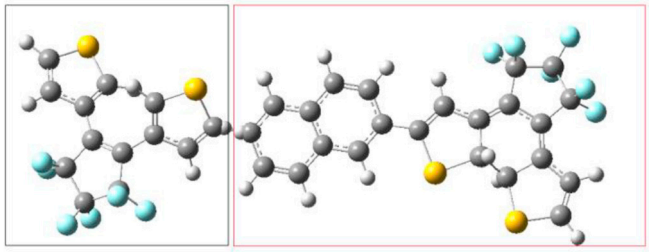

**5oc**

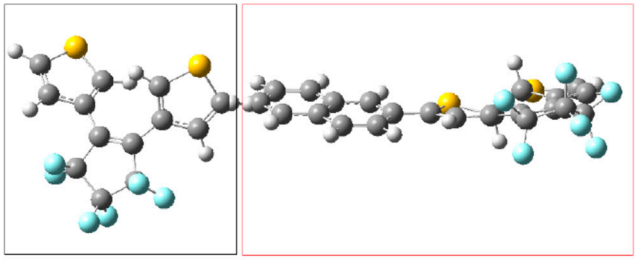

**6oc**

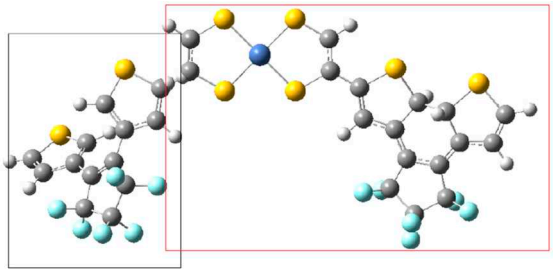

**7oc**

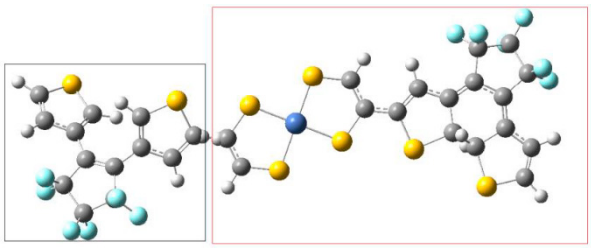

**8oc**

Preprints (www.preprints.org) | NOT PEER-REVIEWED | Posted: 7 July 2023 doi:10.20944/preprints202307.0483.v1



**Figure 3.** The considered dimers (left fragment: donor; right fragment: acceptor.

III. 3A. Intra-molecular excited energy transfer

For the study of the intra-molecular EET (excited energy transfer) we have employed the following approaches:

(i)Two methods have been used for the computation, of $V_{DA}$ of several models, that is the coupling between the donor (open unit) and the acceptor (closed unit). (ii) For the case of **1oc** isomer, the emission spectrum of the donor andthe absorption spectrum of the acceptor have been analyzed.

**A.** In the following section we will discuss the results, obtained by the two methods we have used to calculate $V_{DA}$.

*Linear response method.* The ground state equilibrium geometries have been used to compute $V_{DA}$.[1] We have employed three types of molecular bridges, NiBDT, naphthalene and an oligothiophene (Figures 1–3). For NiBDT and naphthalene, the cis and trans isomers of the corresponding derivative have been considered. For the trans isomer of naphthalene, as a bridge, we have used two conformations, one is planar and in the other, the plane of naphthalene is vertical to the plane of DTE groups. NiBDT is bonded with the two switches with two different ways: (i) NiBDT is fused with the two DTE units (**2oc**; Figure 2) and (ii) it is bonded with the switches with single bonds (**7oc** & **8oc**; Figure 3). Each molecule is decomposed into two fragments: D (donor; the open DTE) and A (acceptor; the closed DTE bonded with the bridge ). The bond, which is cut is capped with a hydrogen atom at both ends. Thus, a well-defined fragment results. The employed models are given in Figure 3. The linker (or bridge), i.e naphthalene, NiBDT, oligothiophene is bonded to the closed DTE unit (acceptor). This model corresponds to the M2 one employed by Fihey et al.[1] It has been selected because it was found in ref [1] when the bridge is bonded to the acceptor unit the Coulomb interaction is enhanced and thus a significant EET process takes place. A detailed discussion of this and several other models is given in the above reference. For the computation of $V_{DA}$ one needs to find the excited states, which participate in the EET process.[1] For the open DTE moiety, which is the donor fragment, the excited state involves, in most cases, a HOMO-LUMO transition; this is connected with the photocyclization process. Thus, the selected relevant transition energy should lie in the UV region. The relevant excited state of the closed DTE unit, which is the acceptor -fragment, is selected by taking into account two criteria: (i) its energy should be close and lower than the energy of the donor and (ii) it should have a non-negligible oscillator strength. It has been shown, based on the Förster's theory that a significant suppression of the EET rate takes place, when the excitation energy difference between the donor and the acceptor is large, in comparison with other relevant energy properties of the interacting molecules.*[93]* Table 10 reports two contributions to $V_{DA}$: the coulombic ($V_c$) and the exchange ($V_{xc}$).

**Table 10.** Electronic couplings ($V_{DA}$) and different contributions ($V_c$, $V_{xc}$) for the considered dimers. All values are given in $cm^{-1}$. All values were computed with CAM-B3LYP/6-31G* method.

| Dimer | $V_{DA}$ | $V_c$ | $V_{xc}$ |
|---|---|---|---|
| **1oc**[a] | 8.3 | 8.1<br>9,7[b] | 0.2<br>0.25[b] |
| **2oc** | 10,3 | 9,7 | 0,6 |
| **4oc** | 101.5 | 101.6 | -0.1 |
| **5oc** | 113.0 | 111.3 | 1.7 |
| **6oc** | 120.4 | 120.9 | -0.5 |
| **7oc** | 32.3 | 30.9 | 1.4 |
| **8oc** | 12.8 | 12.1 | 0.7 |

[a] R=Cl (Fig. 1).[b] Properties have been computed at the M062-X optimized geometry.

Areephong et al.[53] observed ring closure of both photochromic units for the sexithiophenes they studied (**1oc**; Figure 1; R: Cl). In agreement with the experimental observation, a low value of $V_{DA}$ was computed for R=Cl, (8.3 $cm^{-1}$; Table 11) suggesting ring closure,. In the second derivative

Preprints (www.preprints.org) | NOT PEER-REVIEWED | Posted: 7 July 2023 doi:10.20944/preprints202307.0483.v1



considered (**2oc**; Figure 2), each DTE group is fused with two NiBDT molecules, while the Ni compound also operates as a bridge. A rather low $V_{DA}$ has been computed for this (10.3 $cm^{-1}$). Therefore, if we consider this value of $V_{DA}$ (8.3 $cm^{-1}$) as a reference, it is likely that NiBDT bridge allows the switching between the three states, although for a more complete answer other factors should also be considered (e.g energy transfer speed, cyclisation time).[1]

**Table 11.** Electronic transition energies(E;eV) and oscillator strengths (f).

| Dimer | $D_n$[a] | E/f[b] | Transition/(%) | $A_n$[a] | E/f[b] | Transition/(%) |
|---|---|---|---|---|---|---|
| **1oc**[c] | $D_1$ | **4.433/0.139**<br>**4.450/0.111**[d] | **HOMO->LUMO/(100)** | **$A_7$** | **4.233/0.04**<br>**4.320/0.01**[d] | **HOMO-2->LUMO/21**<br>**HOMO-1->LUMO+4/19**<br>**HOMO->LUMO+4/27** |
| **2oc** | **$D_{22}$** | **4,619/0,22** | HOMO-14->LUMO (50%)<br>HOMO->LUMO+2 (12.5%)<br>HOMO-5->LUMO+1 (14.5%) | **$A_{55}$** | **4,607/0,04** | HOMO->LUMO+9(22%)<br>HOMO-9->LUMO+4 (11%)<br>HOMO-7->LUMO+3(5,8%)<br>HOMO-1->LUMO+5(8%) |
| **4oc** | **$D_1$** | **4.226/0.702** | **HOMO->LUMO/(98)** | **$A_4$**<br>$A_1$<br>**$A_2$** | **4.176/0.124**<br>2.628/0.458<br>3.892/0.121 | HOMO->LUMO+1/67<br>HOMO->LUMO/95<br>HOMO-1->LUMO/54<br>HOMO-2->LUMO+1/32 |
| **5oc** | **$D_1$** | **4.217/0.181** | **HOMO->LUMO/(98)** | **$A_4$**<br>$A_1$<br>$A_2$<br>$A_3$ | **4.209/0.356**<br>2.607/0.470<br>3.908/0.108<br>3.921/0.136 | HOMO->LUMO+1/63<br>HOMO->LUMO/100<br>HOMO-2->LUMO/84<br>HOMO-1->LUMO/77 |
| **6oc** | **$D_1$** | **4.217/0.702** | **HOMO->LUMO/(98)** | **$A_4$**<br>$A_1$<br>$A_2$<br>$A_3$ | **4.210/0.356**<br>2.607/0.689<br>3.909/0.108<br>3.921/0.136 | HOMO->LUMO+1/63<br>HOMO->LUMO/100<br>HOMO-2->LUMO/84<br>HOMO-1->LUMO/77 |
| **7oc** | $D_1$<br>$D_2$<br>$D_3$<br>**$D_4$** | 2.482/0<br>3.147/0<br>3.627/0<br>**4.231/0.174** | **HOMO->LUMO/(100)** | $A_6$<br>$A_{24}$<br>$A_{42}$<br>$A_{46}$<br>**$A_{50}$** | 1.345/0.37<br>2.650/0.28<br>3.770/0.15<br>4.040/0.06<br>**4.160/0.06** | HOMO->LUMO/92<br>HOMO->LUMO+1/84<br>HOMO-1->LUMO+1/79<br>HOMO-2->LUMO+1/84<br>**HOMO-6->LUMO/29**<br>**HOMO-14->LUMO/25**<br>**HOMO-3->LUMO/8** |
| **8oc** | $D_1$<br>$D_2$<br>$D_3$<br>**$D_4$** | 2.456/0<br>3.140/0<br>3.620/0<br>**4.205/0.173** | **HOMO->LUMO/(100)** | $A_6$<br>$A_7$<br>$A_{24}$<br>$A_{32}$<br>$A_{40}$<br>$A_{47}$<br>**$A_{50}$** | 1.383/0.51<br>2.607/0.02<br>2.600/0.215<br>3.109/0.04<br>3.730/0.141<br>4.095/0.06<br>**4.136/0.01** | HOMO->LUMO/92<br>HOMO-1->LUMO/79<br>HOMO->LUMO+1/87<br>HOMO-2->LUMO/44<br>HOMO-1->LUMO+1/79 |

Preprints (www.preprints.org) | NOT PEER-REVIEWED | Posted: 7 July 2023 doi:10.20944/preprints202307.0483.v1



| | |
|---|---|
| | **HOMO-2->LUMO+1/40 HOMO->LUMO+2/37** |

[a] $D_n/A_n$: n denotes the number of Donor/Acceptor state for the transition $S_0$->$S_n$.[b] E/f: Electronic Transition Energy(eV)/Oscillator Strength. [c] R=Cl (Figure 1). [d] Properties have been computed at the M062-X optimized geometry.

We observe that for **2oc** the relevant excited state of the donor is the 22nd (268 nm; Table 11). This is, of course, quite high and reinforces the conjecture of a very low probability of EET. Nevertheless, although it is known that the higher-energy emission bands in the UV would violate Kasha's rule and Kasha–Vavilov rule for fluorescence, violations of these rules are reported specifically in connection with intramolecular EET.[94–97] Figure 4 presents the emission spectrum of the fragment, which operates as donor, the absorption spectrum of the fragment, which acts as acceptor and their overlap. The emission, which is relevant for EET is found in the area 230-300nm. We observe two peaks at 250 nm and 270 nm. However, two antagonistic processes are likely to take place before EET proceeds: internal conversion to $S_1$ and photo-cyclization of the open DTE group. In addition, all the oscillator strength (*f*) values, associated with the emission in UV, except that of the 22nd state are negligible (Table 3S). Taking into account these considerations and the corresponding small value of $V_{AD}$ (10.3 $cm^{-1}$), we believe that EET is unlikely to take place and thus the open DTE unit of **2oc** is likely to close.

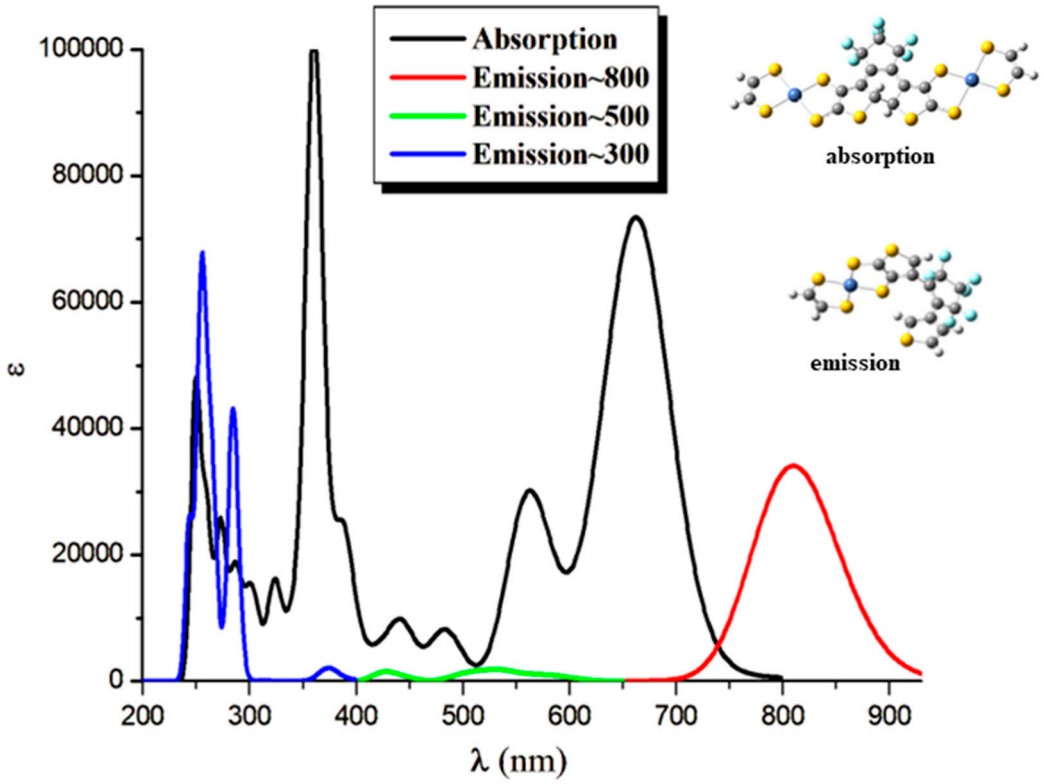


**Figure 4.** The absorption (black line) and the emission spectra (red, green, blue lines) of the **2oc** fragments (left fragment: Donor, right fragment: Acceptor). The CAMB3LYP/6-31G* method was used.

**4oc**, **5oc** and **6oc** have naphthalene as a linker; **4oc** involves the DTE groups in cis orientation, while **5oc** and **6oc** have the DTE units in trans orientations. In **5oc** and **6oc** the naphthalene groups have a different arrangement (Figure 3). In all considered cases $V_{xc}$ is very small. We observe that $V_{DA}$ is very large for **4oc**-**6oc,** where naphthalene is the linker. This suggests significant EET and thus,

Preprints (www.preprints.org) | NOT PEER-REVIEWED | Posted: 7 July 2023 doi:10.20944/preprints202307.0483.v1



partial photochromic activity (i.e. the closing of only one photochromic unit is likely to be observed). The significant effect of geometry on $V_{DA}$ is clearly demonstrated by these results (Table 10).

**7oc** and **8oc** involve NiBDT as a linker. **7oc** and **8oc** have the DTE groups in cis and trans orientation, respectively. We observe that for **7oc** and **8oc** the excited states, $S_1 - S_3$ , of the donor have for emission *f=0*. Thus $S_4$ was considered. The smaller $V_{DA}$ is observed for the trans isomer, **8oc** (12.8cm$^{-1}$). This low $V_{DA}$ suggests that no significant EET takes place, therefore, both DTE groups are likely to close.

It is interesting to compare the $V_{DA}$ (Coulomb contribution, $V_C$) value of naphthalene as a linker with that of a biphenyl group as a bridge. In the first case $V_C$ = 101.6-120.9 cm$^{-1}$, depending on the orientation of the open/closed units of the linker; in naphthalene the two phenyl groups are fused. In the second case, $V_{DA}$ = 3.1cm$^{-1}$; the two phenyl groups are connected with a single bond. The great effect of the structure on $V_{DA}$ is clearly seen.

We observe that for **5oc** (Table 11, Figure 3) the transition energy for the acceptor, 4.209eV is associated with the 4$^{th}$ excited state, $S_4$. However, for **8oc**, the corresponding transition energy 4.136 eV is associated with the excited state $S_{50}$. This very large number of intervening excited states is due to the presence of NiBDT.[90] The unusually large NLO properties of NiBDT derivatives (Table 2) are also due to the significant number of low-lying excited states.

The calculation of $V_{DA}$, by the linear response method, illuminates some aspects of EET, that is the excitation of the open DTE and the absorption of the closed DTE, which is due to the de-excitation of the open DTE.

Our results clearly show that the linker strongly influences the communication between the DTE groups and thus, photochromism. The molecular geometry has a significant effect on $V_{DA}$. NiBDT, as a linker, is associated with, relatively, low $V_{DA}$ values; therefore both DTE groups are likely to close. This low $V_{DA}$ is due to the near-IR absorption spectrum of NiBDT. Our computations have shown that the considered oligothiophene, as a linker, is associated with low $V_{DA}$ and thus allows both DTE groups to close. This is in agreement with the experimental observation.[53]

*Distributed multipole analysis (DMA).* To gain a further understanding of the EET process we have also computed the $V_c$ contribution of $V_{DA}$ by the method proposed by Błasiak, et al.,[81] which relies on the distributed multipole expansion of the transition densities. The results for the DMA treatment, as a function of the limiting value of the sum of the interacting multipole moments $l+l'$ (where $l,l'$=0 (charge), ... , 4 (hexadekapole)) are given in Table 12. It has been shown in Ref. [[81]], and was also found here, that limiting the sum of the ranks yields better results than the alternative approach of using all multipoles up to a limiting rank $l$. *As the values show, the electrostatic contribution computed using the multipole expanded transition density employing the highest limiting rank $l+l' = 4$ compare quite well with the analytically computed values (linear response method)*; the differences are in the range of $10^{-4}$ eV (~ 0.8cm$^{-1}$). We note that both the added terminal hydrogen $H_{term}$ as well as the carbon atom connected with it were not used as explicit expansion centers in the DMA treatment. The remaining differences between the multipole-expanded method and the analytical values may be caused at least in part by a not yet converged expansion series and/or by the charge density of $H_{term}$, which has not been removed. Although $H_{term}$ was not used as an expansion center, its associated charge density is still taken into account in the DMA treatment.

We concluded that the results for $V_c$, computed with the DMA method, are in satisfactory agreement with those calculated with the linear response approach (Tables 10 and 12).

**Table 12.** Comparison of the Coulomb-term contribution to the total EET, computed using a multipole expansion of the transition density, with analytically computed values; all values are in cm$^{-1}$( ~$10^{-4}$eV).

| l+l′ Bridge | 0 | 1 | 2 | 3 | 4 | Analyt. Coulomb[a] | Analyt. EET[a.] |
|---|---|---|---|---|---|---|---|
| Naphthalene | 82.3 | 137.1 | 143.6 | 127.4 | 117.8 | 111.3 | 112.9 |
| NiBDT | 4.8 | 8.1 | 13.7 | 12.1 | 15.3 | 12.1 | 12.9 |

Preprints (www.preprints.org) | NOT PEER-REVIEWED | Posted: 7 July 2023 doi:10.20944/preprints202307.0483.v1



[a] The distributed multipole moments are computed analytically (using, in our case, Stones' GDMA method) in contrast to the 'fitting' procedures used by other approaches, which fit the multipole moments to the external charge density.

III. 3.B Overlap of the emission spectrum of the donor and the absorption spectrum of the acceptor

In this section we shall discuss the overlap of the emission spectrum of the donor and the absorption spectrum of the acceptor. The considered systems involve **2oo**, **2oc** and **2cc** (Figure 2), where for the pair **2oo/2oc**, **2oo** is the donor and **2oc** is the acceptor, i.e., **2oo** absorbs photons and then emits, while the **2oc** absorbs the emitted photons. Similarly, for the pair **2oc/2cc**, **2oc** is the donor and **2cc** is the acceptor, i.e., **2oc** which had absorbed photons, it emits, while the **2cc** absorbs the emitted photons. This overlap is an indication that EET phenomenon may occurs between different molecules. Of particular relevance for this work is overlap in the UV area, because photo-cyclization takes place at this area. One of our major themes is whether EET will allow the open DTE unit of **2oc** to close leading to **2cc**.

For the case of the **2oo** structure, two conformers **a** and **b** have been obtained. Rotations around C-C bond convert **a** isomer to **b**, see Figure 5. The **a** conformer is lowest in energy than **b** by 0.18 eV because weak π-π interactions are formed between the rings of the central NiBDT and the rings of the other NiBDT groups. However, both present similar absorption spectra, i.e., their peaks differ less than 6 nm and up to 0.03 eV, see below. Finally, it should be mentioned that the optimized geometry of the excited states of **2oo,** that corresponds to the main peaks of the emission spectra, have similar geometry with **b**.

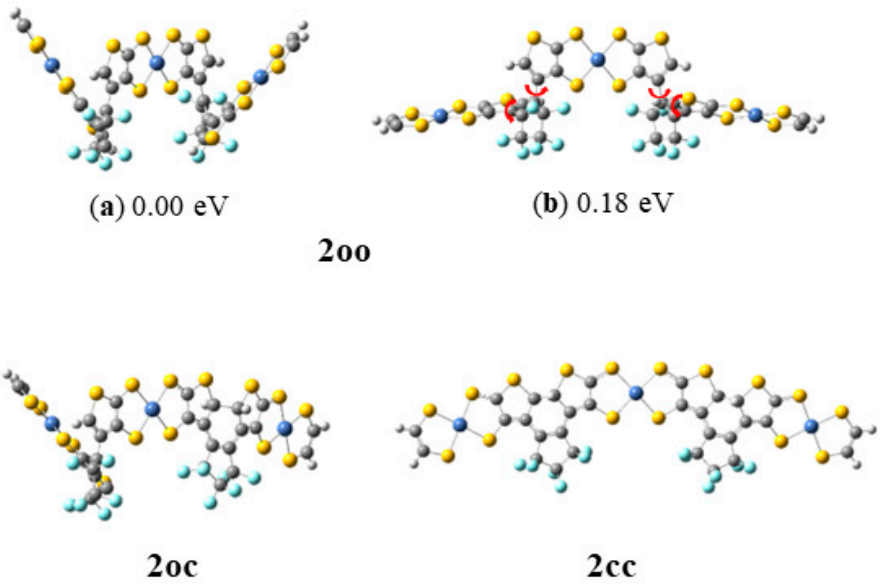


**Figure 5.** Calculated open-open (**2oo**), open-closed (**2oc**) and closed-closed (**2cc**) structures at CAM-B3LYP/6-31G*$_{H,C,O,F,S}$ ECP28MWB(SDD)$_{Ni}$.

Preprints (www.preprints.org) | NOT PEER-REVIEWED | Posted: 7 July 2023 doi:10.20944/preprints202307.0483.v1



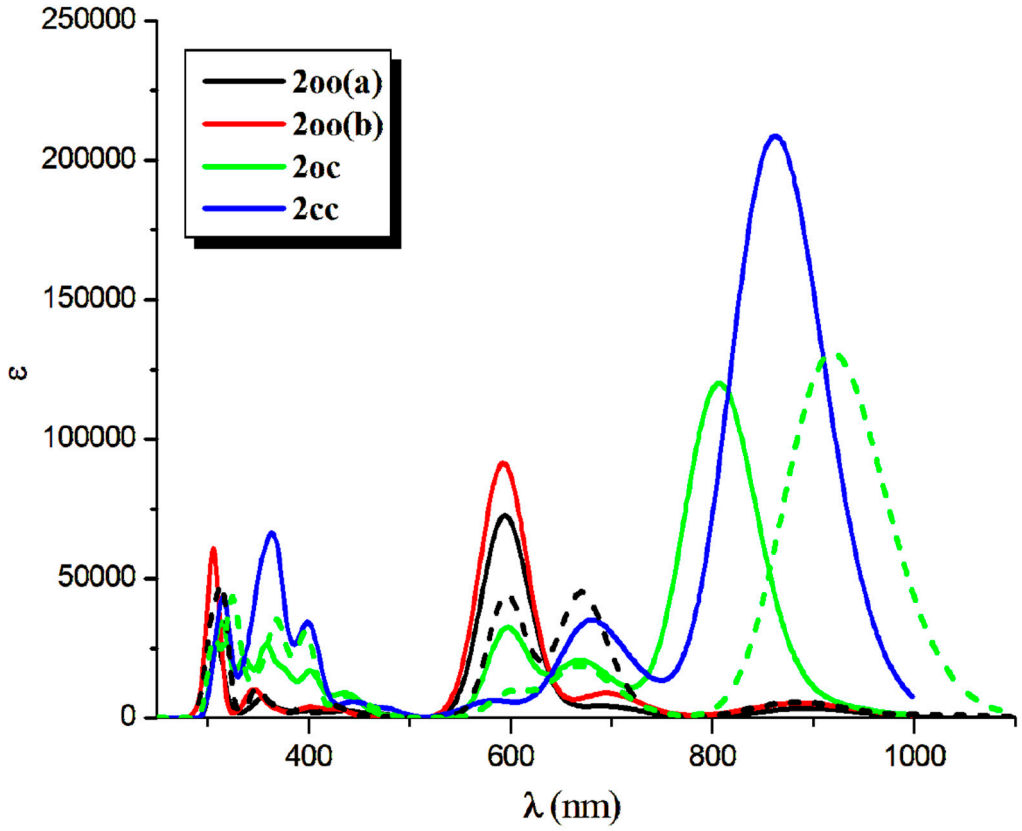


**Figure 6.** NIR-vis-UV absorption (solid line) and emission (dotted line) spectra of the **2oo**, **2oc**, and **2cc** structures at CAM-B3LYP/6-31G*$_{H,C,O,F,S}$ ECP28MWB(SDD)$_{Ni}$ level of theory. (Peak half-width at half height: 0.09 eV).

The absorption spectrum of **2oo** has a main peak in the visible range at ~600 nm, an intense peak in UV area at ~310 nm and small overlapping peaks at ~700 nm and ~900 nm in NIR area. On the contrary, the main peak of the absorption spectra of **2oc** and **2cc** is found at 807 and 862 nm in NIR area. At 650 and 600 nm there are some overlapping peaks for the **2oc** and at 670 nm for the **2cc**. Finally, both present small peaks in the UV area of 400-300 nm, see figure 6 and figures 4S-5S, Table 13 and Table 4S of SI. The emission spectrum of **2oo** presents two peaks of similar intensity at 670 nm and 313 nm in the vis and UV regions, respectively. The emission spectrum of **1oc** presents three peaks: an intent at 917 nm in the NIR region and two peaks of similar intensity at 662 nm and 326 nm in vis and UV area.

**Table 13.** Excitation energies, ΔE (eV), $\lambda_{max}$ (nm), and f-values for the main peak of the absorption and emission spectra and the corresponding main excitations of the **2oo**, **2oc**, and **2cc** structures at CAM-B3LYP/6-31G*$_{H,C,O,F,S}$ ECP28MWB(SDD)$_{Ni}$ level of theory.

| Struct | ΔE | $\lambda_{max}$ | f | Excitations |
|---|---|---|---|---|
| | | | **Absorption** | |
| **2oo(a)** | 1.805 | 686.9 | 0.0115 | 0.35\|H-2 L+1> – 0.29\|H L+2> + 0.28\|H-1 L+1> + 0.26\|H-2 L> |
| | 2.071 | 598.7 | 0.1141 | 0.20\|H L+2> + 0.16\|H-1 L+2> – 0.21\|H-10 L+5> |
| | 4.006 | 309.5 | 0.1252 | 0.19\|H-6 L+2> – 0.13\|H-1 L+6> |
| **2oo(b)** | 1.791 | 692.2 | 0.0447 | 0.56\|H-1 L+1> – 0.36\|H L+2> |
| | 2.088 | 593.7 | 0.4031 | 0.42\|H L+2> + 0.23\|H-1 L+1> – 0.18\|H-2 L> |

Preprints (www.preprints.org) | NOT PEER-REVIEWED | Posted: 7 July 2023 doi:10.20944/preprints202307.0483.v1



| | | | | |
|---|---|---|---|---|
| | 4.044 | 306.6 | 0.2014 | 0.18\|H-2 L+8> + 0.20\|H-5 L+2> – 0.22\|H-35 L> – 0.20\|H-19 L+3> |
| **2oc** | 1.537 | 806.9 | 0.7112 | 0.58\|H L> – 0.23\|H-5 L> |
| | 1.868 | 663.7 | 0.0926 | 0.38\|H-2 L> – 0.27\|H-5 L> |
| | 3.925 | 315.9 | 0.0983 | 0.39\|H-17 L> + 0.22\|H-26 L> +0.31\|H-26 L+2> |
| **2cc** | 1.438 | 862.3 | 1.3931 | 0.51\|H L> + 0.30\|H-1 L+1> |
| | 1.837 | 675.1 | 0.1866 | 0.23\|H L+4> + 0.20\|H-4 L> – 0.23\|H-2 L+1> + 0.18\|H-1 L> |
| | 3.107 | 399.0 | 0.1077 | 0.28\|H-1 L+1> + 0.21\|H L+4> – 0.21\|H-4 L+1> – 0.18\|H-4 L> |
| | 3.369 | 368.0 | 0.1701 | 0.29\|H-17 L> – 0.16\|H-18 L> + 0.15\|H-8 L> |
| | 3.519 | 352.4 | 0.1073 | 0.27\|H-19 L+1> + 0.19\|H-19 L> – 0.18\|H-9 L+1> – 0.11\|H-2 L+1> |
| | 3.917 | 316.5 | 0.1402 | 0.27\|H-16 L+1> + 0.21\|H-16 L>– 0.19\|H-13 L> + 0.26\|H-5 L> |
| | | | **Emission** | |
| **2oo** | 1.444 | 858.7 | 0.0170 | 0.65\|H-4 L> – 0.15\|H-2 L> |
| | 1.851 | 669.7 | 0.1938 | 0.47\|H-1 L+2> – 0.51\|H-1 L+1> – 0.39\|H-14 L+2>+ 0.27\|H-12 L+2> + 0.21\|H-14 L+1> |
| | 2.074 | 597.8 | 0.1588 | 0.52\|H L+2> + 0.40\|H-9 L+4> |
| | 3.966 | 312.6 | 0.2401 | 0.33\|H-2 L+8> + 0.14\|H-2 L+6> – 0.36\|H-34 L> |
| **2oc** | 1.353 | 916.5 | 0.7071 | 0.57\|H L> – 0.24\|H-4 L> |
| | 1.874 | 661.6 | 0.0774 | 0.32\|H-5 L> + 0.29\|H L+1> – 0.43\|H-2 L> – 0.25\|H H-19> |
| | 3.806 | 325.8 | 0.0748 | 0.31\|H-15 L> + 0.23\|H-4 L+4> – 0.25\|H-5 L+5> |

The vertical and adiabatic excitation energies with respect to the ground state and the vertical emission de-excitation are shown in Table 14. We found that the absorption spectra of **2oo** presents two main peaks that correspond to excitations of 2.07 and 4.01 eV and a small peak that corresponds to excitations of 1.81. As new rings are formed (**2oo→2oc→2cc**), less energy is needed for these three vertical excitations, i.e., the excitations are red shifted for the **2oc** structure up to 0.3 eV and further red shifted for **2cc**. The most intense red shifted excitation is for the small peak at 1.81 eV and the least red shifted excitation is for the main peak of the 4.01 eV. Similarly, the vertical emission and the adiabatic excitation is similar or less for the **2oc** comparing to **2oo**.

**Table 14.** Vertical and adiabatic excitation energies in eV of the main peaks of the **2oo**, **2oc**, and **2cc** structures at CAM-B3LYP/6-31G*$_{H,C,O,F,S}$ ECP28MWB(SDD)$_{Ni}$.

| 2oo | 2oc | 2cc | 2oo | 2oc | 2oo | 2oc |
|---|---|---|---|---|---|---|
| | $S_0 \rightarrow S_i$ [a] | | | $S_i \rightarrow S_0$ [b] | | $S_0 \rightarrow S_i$ [c] |
| 1.81 (1.79)[d] | 1.54 | 1.44 | 1.44 | 1.35 | 1.67 | 1.40 |
| 2.07 (2.09)[d] | 1.87 | 1.84 | 1.85 | 1.86 | 1.98 | 1.87 |
| 4.01 (4.04)[d] | 3.92 | 3.11 | 3.97 | 3.81 | 4.00 | 3.88 |
| | | 3.37 | | | | |
| | | 3.52 | | | | |
| | | 3.92 | | | | |

[a] Vertical absorption at the geometry of the ground state. [b] Vertical emission at the geometry of the emitted state. [c] Adiabatic excitation. [d] Main peaks of the b structure in parenthesis.

Preprints (www.preprints.org) | NOT PEER-REVIEWED | Posted: 7 July 2023 doi:10.20944/preprints202307.0483.v1



It is of interest that the vertical main emitting peaks of the **2oo** are at 1.44, 1.85, and 3.97 eV, very similar to the absorption peaks of the **2oc** which are at 1.54, 1.87, and 3.92 eV, see Table 14. This shows that energy transfer is possible from the excited open-ring unit to the closed-ring unit, i.e., **2oo→2oc**. Similarly, the vertical main emitting peaks of the **2oc** are at 1.35, 1.86, and 3.81 eV and the adiabatic de-excitation energies are at 1.40, 1.87, and 3.88 eV; and thus, they are very similar to the absorption peaks of the **2cc** which are at 1.44, 1.84, and 3.92 eV. Again, energy transfer is possible from the excited open-ring (**2oc→2cc**) unit to the closed-ring unit. Conclusively, energy transfer is possible through this **2oo→2oc→2cc** process.

The findings of the reported excited state computations are in agreement with the conclusions presented in Ref. 87. The authors there reported that excited-state quenching is responsible for the absence of photochemistry in dithienylethene/sexithiophene-based polymer while intramolecular quenching is observed for the dithienylethene units by the sexithiophene unit.

Finally, the frontier molecular orbitals (MO) involving in the main excitations are depicted in Figures 7-9. It is of interest that many MO orbitals are involved in the main excitations, see Table 4S and Table 13. The main absorption peaks of the **a** conformer in vis and UV area are at 599 nm and 310 nm and they present a small charge transfer (CT) character. This results from the fact that in **a** conformer π-π interactions exist, which are observed in the occupied orbitals, see for instance HOMO and HOMO-6 in Figure 7. In the unoccupied LUMO and LUMO+2 orbitals, where the electron is transferred via the excitation, it is in the peripheral NiBDT group. On the contrary, in the **b** conformer no CT character is observed due to the absence of the π-π interactions. The fluorescence peaks of the **2oo** at 859 nm and 670 nm have not a CT character, however, the peak at 312 nm does, see Figure 7. The three peaks of the absorption spectrum of **2oc** at 807, 664, and 316 nm have only a small partially CT character. The emitting peak at 326 nm is a CT de-excitation from d orbitals of Ni to p electrons of S, see Figure 8. Finally, regarding the **1cc**, where additional aromatic rings are formed, the absorption peak at 317 nm has a clear CT character, with a significant f coefficient of 0.14, from the peripheral $C_2H_2S_2Ni$ group to the whole molecule, i.e., the electron density is delocalized in all **2cc** structure, see Figure 9.

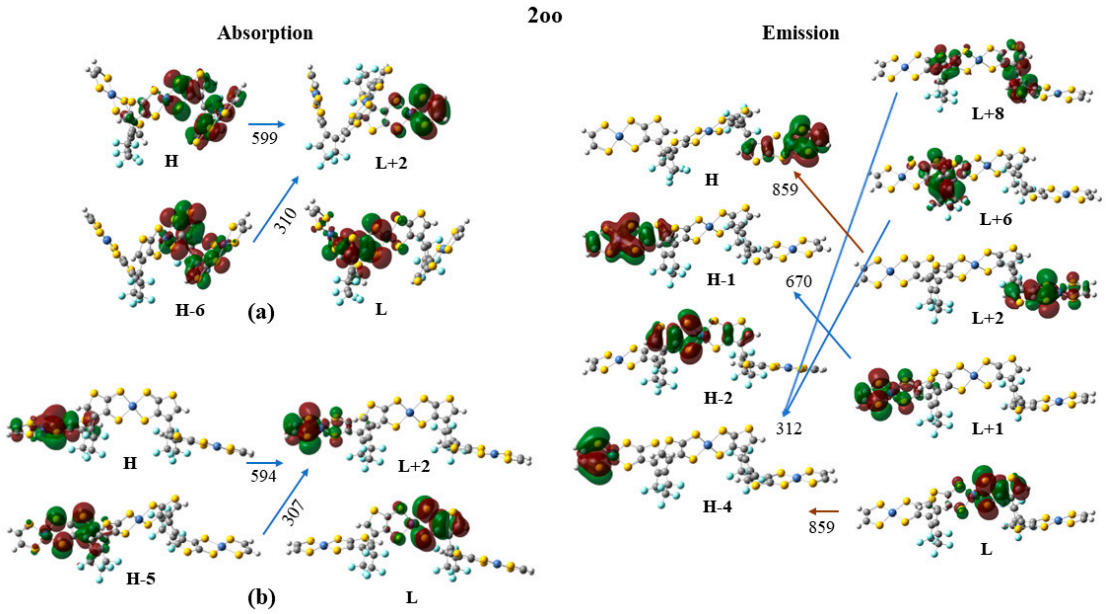


**Figure 7.** Frontier molecular orbitals (MO) involving in the main absorption and emission excitations of **2oo**.

Preprints (www.preprints.org) | NOT PEER-REVIEWED | Posted: 7 July 2023 doi:10.20944/preprints202307.0483.v1



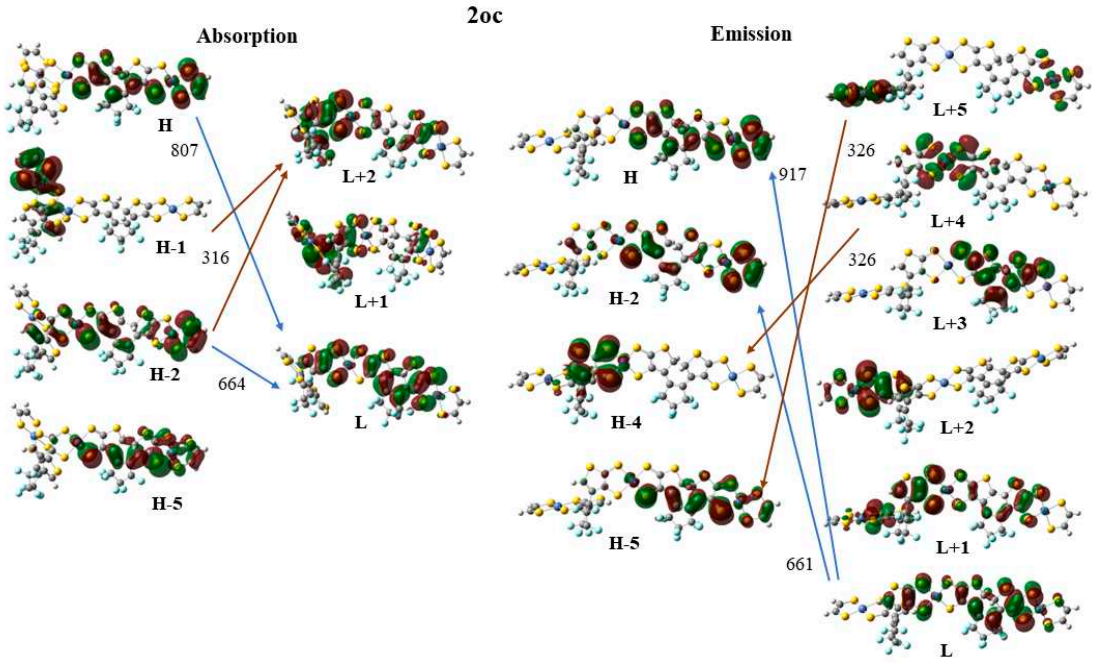


**Figure 8.** Frontier molecular orbitals (MO) involving in the main absorption and emission excitations of **2oc**.

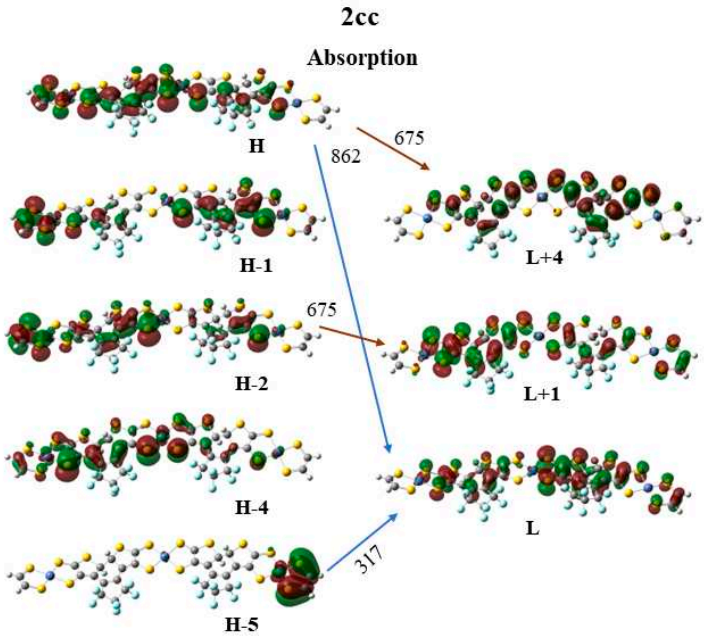


**Figure 9.** Frontier molecular orbitals (MO) involving in the main absorption excitations of **2cc**.

## Conclusions

A significant contrast of the hyperpolarizabilities has been observed between the *open-open*, *open-closed* and the *closed-closed* isomers of the studied compounds. NIBDT, as a linker, is associated with a greater contrast, in comparison to naphthalene, in the properties of interest. This has been attributed to the low lying excited states of NiBDT. As it has been shown, the existence of low lying excited states, due to the presence of NiBDT, significantly enhances the polarization character.

The *closed-closed* isomer clearly demonstrates the great effect of the conjugation on the hyperpolarizabilities. The structural changes induced by photochromism can be closely followed

by the second hyperpolarizability, and thus this property can be used as an index to monitor the molecular changes, which are due to photochromism. A similar trend, although to a lesser extent, has also been found for the first hyperpolarizability. Overall, it is observed that the NLO molecular properties can be used as probes for detection of the possible molecular states.

As expected, we found that the linker greatly affects the communication between the DTE groups and thus, photochromism. It was found that a low $V_{DA}$ is associated with NiBDT as a linker, therefore both DTE groups are likely to close. The near-IR absorption spectrum of NiBDT could be associated with the observed low $V_{DA}$ and the diminished communication. We found that $V_{DA}$ is also affected by the molecular geometry. The computed low $V_{DA}$ value for the case of the sexithiophene, R=Cl, molecular switch is in agreement with the experimentally observed full photochromism [84]. The linear response and the DMA methods give very close electrostatic contributions to $V_{DA}$.

Energy transfer may occur via the **oo→oc→cc** process. The vertical main emitting peaks of the **oo** are very similar to the absorption peaks of the **oc**. Similarly, the vertical main emitting peaks of the **oc** and the adiabatic de-excitation energies are very similar to the absorption peaks of **cc**.

Intramolecularly, the **cc** fragment, presents major absorption peaks at ~650 nm, while the **oo** fragment does not present significant emission in this area. Thus, the bridge does not ease the charge transfer intramolecular from the **o** fragment.

An overlap is observed between the fluorescence spectrum of **oc** with the absorption spectrum of **cc** and between the fluorescence spectrum of **oo** with the absorption spectrum of **oc**. The absorption and emission peaks at ~310 nm in all cases present charge transfer character.

The results of the present study clearly reveal that the electronic nature of the NiBDT molecular bridge, connecting the open-closed DTE units, could allow the photoswitching between molecular states with tunable polarization characteristics. The sensitivity of the L&NLO properties could be used as a probe for the identification of the photoswitching process and the existence of the possible isomers.

**Author Contributions:** Conceptualization: A.A., M.G.P.; investigation: A.A.,D.T. H.R.,R.Z and M.G.P, data curation: : A.A.,D.T. H.R.,R.Z and M.G.P.; writing—original draft: M.G.P.,A.A.,D.T. H.R.,R.Z; writing—review & editing: M.G.P.,A.A., D.T All authors have read and agreed to the published version of the manuscript.

**Acknowledgments:** The authors wish to acknowledge Prof. Denis Jacquemin, Prof. Wesley Browne, Prof. Jan Cz Dobrowolski and Prof. Seiya Kobatake for some helpful and constructive discussions.

## References

1. Fihey, A., R. Russo, L. Cupellini, D. Jacquemin, and B. Mennucci. "Is Energy Transfer Limiting Multiphotochromism? Answers from Ab Initio Quantifications." *Physical Chemistry Chemical Physics* 19, no. 3 (2017): 2044-52.
2. Galanti, A., J. Santoro, R. Mannancherry, Q. Duez, V. Diez-Cabanes, M. Valasek, J. De Winter, J. Cornil, P. Gerbaux, M. Mayor, and P. Samori. "A New Class of Rigid Multi(Azobenzene) Switches Featuring Electronic Decoupling: Unravelling the Isomerization in Individual Photochromes." *Journal of the American Chemical Society* 141, no. 23 (2019): 9273-83.
3. Hsu, C. P. "The Electronic Couplings in Electron Transfer and Excitation Energy Transfer." *Accounts of Chemical Research* 42, no. 4 (2009): 509-18.
4. Nakamura, Y., N. Aratani, and A. Osuka. "Cyclic Porphyrin Arrays as Artificial Photosynthetic Antenna: Synthesis and Excitation Energy Transfer." *Chemical Society Reviews* 36, no. 6 (2007): 831-45.
5. Zhang, L. Y., R. A. Friesner, and R. B. Murphy. "Ab Initio Quantum Chemical Calculation of Electron Transfer Matrix Elements for Large Molecules." *Journal of Chemical Physics* 107, no. 2 (1997): 450-59.
6. Headgordon, M., A. M. Grana, D. Maurice, and C. A. White. "Analysis of Electronic-Transitions as the Difference of Electron-Attachment and Detachment Densities." *Journal of Physical Chemistry* 99, no. 39 (1995): 14261-70.
7. You, Z. Q., C. P. Hsu, and G. R. Fleming. "Triplet-Triplet Energy-Transfer Coupling: Theory and Calculation." *Journal of Chemical Physics* 124, no. 4 (2006).
8. Iozzi, M. F., B. Mennucci, J. Tomasi, and R. Cammi. "Excitation Energy Transfer (Eet) between Molecules in Condensed Matter: A Novel Application of the Polarizable Continuum Model (Pcm)." *Journal of Chemical Physics* 120, no. 15 (2004): 7029-40.

9. Scholes, G. D. "Long-Range Resonance Energy Transfer in Molecular Systems." *Annual Review of Physical Chemistry* 54 (2003): 57-87.
10. Kaieda, T., S. Kobatake, H. Miyasaka, M. Murakami, N. Iwai, Y. Nagata, A. Itaya, and M. Irie. "Efficient Photocyclization of Dithienylethene Dimer, Trimer, and Tetramer: Quantum Yield and Reaction Dynamics." *Journal of the American Chemical Society* 124, no. 9 (2002): 2015-24.
11. Chen, H. C., Z. Q. You, and C. P. Hsu. "The Mediated Excitation Energy Transfer: Effects of Bridge Polarizability." *Journal of Chemical Physics* 129, no. 8 (2008).
12. Scholes, G. D., K. P. Ghiggino, A. M. Oliver, and M. N. Paddonrow. "Through-Space and through-Bond Effects on Exciton Interactions in Rigidly Linked Dinaphthyl Molecules." *Journal of the American Chemical Society* 115, no. 10 (1993): 4345-49.
13. Oevering, H., M. N. Paddonrow, M. Heppener, A. M. Oliver, E. Cotsaris, J. W. Verhoeven, and N. S. Hush. "Long-Range Photoinduced through-Bond Electron-Transfer and Radiative Recombination Via Rigid Nonconjugated Bridges - Distance and Solvent Dependence." *Journal of the American Chemical Society* 109, no. 11 (1987): 3258-69.
14. Pettersson, K., A. Kyrychenko, E. Ronnow, T. Ljungdahl, J. Martensson, and B. Albinsson. "Singlet Energy Transfer in Porphyrin-Based Donor-Bridge-Acceptor Systems: Interaction between Bridge Length and Bridge Energy." *Journal of Physical Chemistry A* 110, no. 1 (2006): 310-18.
15. Cho, H. S., D. H. Jeong, M. C. Yoon, Y. H. Kim, Y. R. Kim, D. Kim, S. C. Jeoung, S. K. Kim, N. Aratani, H. Shinmori, and A. Osuka. "Excited-State Energy Transfer Processes in Phenylene- and Biphenylene-Linked and Directly-Linked Zinc(Ii) and Free-Base Hybrid Diporphyrins." *Journal of Physical Chemistry A* 105, no. 17 (2001): 4200-10.
16. Smith, T. A., N. Lokan, N. Cabral, S. R. Davies, M. N. Paddon-Row, and K. P. Ghiggino. "Photophysics of Novel Donor-{Saturated Rigid Hydrocarbon Bridge}-Acceptor Systems Exhibiting Efficient Excitation Energy Transfer." *Journal of Photochemistry and Photobiology a-Chemistry* 149, no. 1-3 (2002): 55-69.
17. Kroon, J., A. M. Oliver, M. N. Paddonrow, and J. W. Verhoeven. "Observation of a Remarkable Dependence of the Rate of Singlet Singlet Energy-Transfer on the Configuration of the Hydrocarbon Bridge in Bichromophoric Systems." *Journal of the American Chemical Society* 112, no. 12 (1990): 4868-73.
18. El-ghayoury, A., A. Harriman, A. Khatyr, and R. Ziessel. "Intramolecular Triplet Energy Transfer in Metal Polypyridine Complexes Bearing Ethynylated Aromatic Groups." *Journal of Physical Chemistry A* 104, no. 7 (2000): 1512-23.
19. McConnell, H. M. "Intramolecular Charge Transfer in Aromatic Free Radicals." *Journal of Chemical Physics* 35, no. 2 (1961): 508-15.
20. Kudernac, T., S. J. van der Molen, B. J. van Wees, and B. L. Feringa. "Uni- and Bi-Directional Light-Induced Switching of Diarylethenes on Gold Nanoparticles." *Chemical Communications*, no. 34 (2006): 3597-99.
21. Chen, J. X., J. Y. Wang, J. R. He, and X. F. Peng. "Photochromic Properties of Ruthenium Complexes with Dithienylethene-Ethynylthiophene." *Dyes and Pigments* 184 (2021).
22. Chergui, M. "Ultrafast Molecular Photophysics in the Deep-Ultraviolet." *Journal of Chemical Physics* 150, no. 7 (2019).
23. Munoz-Losa, A., C. Curutchet, B. P. Krueger, L. R. Hartsell, and B. Mennucci. "Fretting About Fret: Failure of the Ideal Dipole Approximation." *Biophysical Journal* 96, no. 12 (2009): 4779-88.
24. Beljonne, D., C. Curutchet, G. D. Scholes, and R. J. Silbey. "Beyond Forster Resonance Energy Transfer in Biological and Nanoscale Systems." *Journal of Physical Chemistry B* 113, no. 19 (2009): 6583-99.
25. Kenny, E. P., and I. Kassal. "Benchmarking Calculations of Excitonic Couplings between Bacteriochlorophylls." *Journal of Physical Chemistry B* 120, no. 1 (2016): 25-32.
26. Sauer, K., R. J. Cogdell, S. M. Prince, A. Freer, N. W. Isaacs, and H. Scheer. "Structure-Based Calculations of the Optical Spectra of the Lh2 Bacteriochlorophyll-Protein Complex from Rhodopseudomonas Acidophila." *Photochemistry and Photobiology* 64, no. 3 (1996): 564-76.
27. Krueger, B. P., G. D. Scholes, and G. R. Fleming. "Calculation of Couplings and Energy-Transfer Pathways between the Pigments of Lh2 by the Ab Initio Transition Density Cube Method." *Journal of Physical Chemistry B* 102, no. 27 (1998): 5378-86.
28. Kistler, K. A., F. C. Spano, and S. Matsika. "A Benchmark of Excitonic Couplings Derived from Atomic Transition Charges." *Journal of Physical Chemistry B* 117, no. 7 (2013): 2032-44.
29. Scholes, G. D., and K. P. Ghiggino. "Electronic Interactions and Interchromophore Excitation Transfer." *Journal of Physical Chemistry* 98, no. 17 (1994): 4580-90.
30. Munoz-Losa, A., C. Curutchet, B. P. Krueger, L. R. Hartsell, and B. Mennucci. "Fretting About Fret: Failure of the Ideal Dipole Approximation." *Biophysical Journal* 96, no. 12 (2009): 4779-88.
31. Moerner, W. E. "Viewpoint: Single Molecules at 31: What's Next?" *Nano Lett* 20, no. 12 (2020): 8427-29.
32. Yang, Mino, and Graham R. Fleming. "Third-Order Nonlinear Optical Response of Energy Transfer Systems." *The Journal of Chemical Physics* 111, no. 1 (1999): 27-39.
33. Coe, Benjamin J. "Molecular Materials Possessing Switchable Quadratic Nonlinear Optical Properties." *Chemistry – A European Journal* 5, no. 9 (1999): 2464-71.

34. Castet, Frédéric, Vincent Rodriguez, Jean-Luc Pozzo, Laurent Ducasse, Aurélie Plaquet, and Benoît Champagne. "Design and Characterization of Molecular Nonlinear Optical Switches." *Accounts of Chemical Research* 46, no. 11 (2013): 2656-65.
35. Beaujean, Pierre, Lionel Sanguinet, Vincent Rodriguez, Frédéric Castet, and Benoît Champagne. "Multi-State Second-Order Nonlinear Optical Switches Incorporating One to Three Benzazolo-Oxazolidine Units: A Quantum Chemistry Investigation." *Molecules* 27, no. 9 (2022): 2770.
36. Zhang, J. J., Q. Zou, and H. Tian. "Photochromic Materials: More Than Meets the Eye." *Advanced Materials* 25, no. 3 (2013): 378-99.
37. Boixel, J., A. Colombo, F. Fagnani, P. Matozzo, and C. Dragonetti. "Intriguing Second-Order Nlo Switches Based on New Dte Compounds." *European Journal of Inorganic Chemistry* 2022, no. 12 (2022).
38. Buckingham, A. D. "Permanent and Induced Molecular Moments and Long-Range Intermolecular Forces." In *Advances in Chemical Physics*, 107-42, 1967.
39. Cohen, H. D., and C. C. Roothaan. "Electric Dipole Polarizability of Atoms by Hartree-Fock Method .I. Theory for Closed-Shell Systems." *Journal of Chemical Physics* 43, no. 10 (1965): S034-+.
40. Romberg, W. "Vereinfachte Numerische Intergration." *Kgl. Norske Vid. Selsk. Forsk* 28 (1955): 30-36.
41. Rutishauser, H. " Ausdehnung Des Rombergschen Prinzips." *Num. Math* 5 (1963): 48-54.
42. Davis, P. J., and P. Rabinowitz. *Numerical Intergration*. London: Blaisdell, 1967.
43. Takamuku, Shota, and Masayoshi Nakano. "Theoretical Study on Second Hyperpolarizabilities of Intramolecular Pancake-Bonded Diradicaloids with Helical Scaffolds." *ACS Omega* 4, no. 2 (2019): 2741-49.
44. Frisch, M. J., G. W. Trucks, H. B. Schlegel, G. E. Scuseria, M. A. Robb, J. R. Cheeseman, G. Scalmani, V. Barone, G. A. Petersson, H. Nakatsuji, X. Li, M. Caricato, A. V. Marenich, J. Bloino, B. G. Janesko, R. Gomperts, B. Mennucci, H. P. Hratchian, J. V. Ortiz, A. F. Izmaylov, J. L. Sonnenberg, Williams, F. Ding, F. Lipparini, F. Egidi, J. Goings, B. Peng, A. Petrone, T. Henderson, D. Ranasinghe, V. G. Zakrzewski, J. Gao, N. Rega, G. Zheng, W. Liang, M. Hada, M. Ehara, K. Toyota, R. Fukuda, J. Hasegawa, M. Ishida, T. Nakajima, Y. Honda, O. Kitao, H. Nakai, T. Vreven, K. Throssell, J. A. Montgomery Jr., J. E. Peralta, F. Ogliaro, M. J. Bearpark, J. J. Heyd, E. N. Brothers, K. N. Kudin, V. N. Staroverov, T. A. Keith, R. Kobayashi, J. Normand, K. Raghavachari, A. P. Rendell, J. C. Burant, S. S. Iyengar, J. Tomasi, M. Cossi, J. M. Millam, M. Klene, C. Adamo, R. Cammi, J. W. Ochterski, R. L. Martin, K. Morokuma, O. Farkas, J. B. Foresman, and D. J. Fox. *Gaussian 16 Rev. B.01,Gaussian, Inc., Wallingford CT* (2016).
45. Becke, A. D. "A New Mixing of Hartree-Fock and Local Density-Functional Theories." *Journal of Chemical Physics* 98, no. 2 (1993): 1372-77.
46. Serrano-Andres, L., A. Avramopoulos, J. Li, P. Labeguerie, D. Begue, V. Kello, and M. G. Papadopoulos. "Linear and Nonlinear Optical Properties of a Series of Ni-Dithiolene Derivatives." *Journal of Chemical Physics* 131, no. 13 (2009): 134312.
47. Avramopoulos, A., H. Reis, G. A. Mousdis, and M. G. Papadopoulos. "Ni Dithiolenes - a Theoretical Study on Structure-Property Relationships." *European Journal of Inorganic Chemistry* 2013, no. 27 (2013): 4839-50.
48. Avramopoulos, A., H. Reis, N. Otero, P. Karamanis, C. Pouchan, and M. G. Papadopoulos. "A Series of Novel Derivatives with Giant Second Hyperpolarizabilities, Based on Radiaannulenes, Tetrathiafulvalene, Nickel Dithiolene, and Their Lithiated Analogues." *Journal of Physical Chemistry C* 120, no. 17 (2016): 9419-35.
49. Avramopoulos, Aggelos, Robert Zaleśny, Heribert Reis, and Manthos G. Papadopoulos. "A Computational Strategy for the Design of Photochromic Derivatives Based on Diarylethene and Nickel Dithiolene with Large Contrast in Nonlinear Optical Properties." *The Journal of Physical Chemistry C* 124, no. 7 (2020): 4221-41.
50. Sutradhar, T., and A. Misra. "The Role of Pi-Linkers and Electron Acceptors in Tuning the Nonlinear Optical Properties of Bodipy-Based Zwitterionic Molecules." *Rsc Advances* 10, no. 66 (2020): 40300-09.
51. Cao, L. L., and U. Ryde. "Influence of the Protein and Dft Method on the Broken-Symmetry and Spin States in Nitrogenase." *International Journal of Quantum Chemistry* 118, no. 15 (2018).
52. Garcia-Borras, M., M. Sola, J. M. Luis, and B. Kirtman. "Electronic and Vibrational Nonlinear Optical Properties of Five Representative Electrides." *Journal of Chemical Theory and Computation* 8, no. 8 (2012): 2688-97.
53. Areephong, Jetsuda, Johannes H. Hurenkamp, Maaike T. W. Milder, Auke Meetsma, Jennifer L. Herek, Wesley R. Browne, and Ben L. Feringa. "Photoswitchable Sexithiophene-Based Molecular Wires." *Organic Letters* 11, no. 3 (2009): 721-24.
54. Jacquemin, Denis, Antoine Femenias, Henry Chermette, Ilaria Ciofini, Carlo Adamo, Jean-Marie André, and Eric A. Perpète. "Assessment of Several Hybrid Dft Functionals for the Evaluation of Bond Length Alternation of Increasingly Long Oligomers." *The Journal of Physical Chemistry A* 110, no. 17 (2006): 5952-59.
55. Yanai, T., D. P. Tew, and N. C. Handy. "A New Hybrid Exchange-Correlation Functional Using the Coulomb-Attenuating Method (Cam-B3lyp)." *Chemical Physics Letters* 393, no. 1-3 (2004): 51-57.

56. Francl, M.M., W.J. Pietro, W.J. Hehre, M.S Gordon, DeFees D.J., and J.A Pople. "Self-Consistent Molecular Orbital Methods. Xxiii. A Polarization-Type Basis Set for Second-Row Elements " *Journal of Chemical Physics* 77, no. 7 (1982): 3654-65.
57. Hariharan, P.C., and J.A. Pople. "The Influence of Polarization Functions on Molecular Orbital Hydrogenation Energies." *Theoretica Chimica Acta* 28, no. 3 (1973): 213-22.
58. Dunning, T. H. "Gaussian-Basis Sets for Use in Correlated Molecular Calculations .1. The Atoms Boron through Neon and Hydrogen." *Journal of Chemical Physics* 90, no. 2 (1989): 1007-23.
59. Woon, D. E., and T. H. Dunning. "Gaussian-Basis Sets for Use in Correlated Molecular Calculations .3. The Atoms Aluminum through Argon." *Journal of Chemical Physics* 98, no. 2 (1993): 1358-71.
60. Dolg, M., U. Wedig, H. Stoll, and H. Preuss. "Energy-Adjusted Abinitio Pseudopotentials for the 1st-Row Transition-Elements." *Journal of Chemical Physics* 86, no. 2 (1987): 866-72.
61. Bachler, V., G. Olbrich, F. Neese, and K. Wieghardt. "Theoretical Evidence for the Singlet Diradical Character of Square Planar Nickel Complexes Containing Two Omicron-Semiquinonato Type Ligands." *Inorganic Chemistry* 41, no. 16 (2002): 4179-93.
62. Tzeli, Demeter, Giannoula Theodorakopoulos, Ioannis D. Petsalakis, Dariush Ajami, and Julius Rebek, Jr. "Conformations and Fluorescence of Encapsulated Stilbene." *Journal of the American Chemical Society* 134, no. 9 (2012): 4346-54.
63. Tzeliou, Christina Eleftheria, and Demeter Tzeli. "3-Input and Molecular Logic Gate with Enhanced Fluorescence Output: The Key Atom for the Accurate Prediction of the Spectra." *Journal of Chemical Information and Modeling* 62, no. 24 (2022): 6436-48.
64. Peach, Michael J. G., Peter Benfield, Trygve Helgaker, and David J. Tozer. "Excitation Energies in Density Functional Theory: An Evaluation and a Diagnostic Test." *The Journal of Chemical Physics* 128, no. 4 (2008): 044118.
65. Dreuw, A., and M. Head-Gordon. "Single-Reference Ab Initio Methods for the Calculation of Excited States of Large Molecules." *Chemical Reviews* 105, no. 11 (2005): 4009-37.
66. Casida, M. E., and M. Huix-Rotllant. "Progress in Time-Dependent Density-Functional Theory." *Annual Review of Physical Chemistry, Vol 63* 63 (2012): 287-323.
67. Jacquemin, D., E. A. Perpete, G. E. Scuseria, I. Ciofini, and C. Adamo. "Td-Dft Performance for the Visible Absorption Spectra of Organic Dyes: Conventional Versus Long-Range Hybrids." *Journal of Chemical Theory and Computation* 4, no. 1 (2008): 123-35.
68. Jacquemin, D., A. Planchat, C. Adamo, and B. Mennucci. "Td-Dft Assessment of Functionals for Optical 0-0 Transitions in Solvated Dyes." *Journal of Chemical Theory and Computation* 8, no. 7 (2012): 2359-72.
69. Mahr, H. "Two-Photon Absorption Spectroscopy." In *Quantum Electronics*, edited by H. Rabin and C. L. Tang, 494. New York: Academic Press, 1975.
70. R L Swofford, and, and A C Albrecht. "Nonlinear Spectroscopy." *Annual Review of Physical Chemistry* 29, no. 1 (1978): 421-40.
71. Bloembergen, Nicolaas. *Nonlinear Optics*, Nonlinear Optics, 1996.
72. Olsen, Jeppe, and Poul Jo/rgensen. "Linear and Nonlinear Response Functions for an Exact State and for an Mcscf State." *The Journal of Chemical Physics* 82, no. 7 (1985): 3235-64.
73. Monson, P. R., and W. M. McClain. "Polarization Dependence of the Two-Photon Absorption of Tumbling Molecules with Application to Liquid 1-Chloronaphthalene and Benzene." *The Journal of Chemical Physics* 53, no. 1 (1970): 29-37.
74. Beerepoot, Maarten T. P., Daniel H. Friese, Nanna H. List, Jacob Kongsted, and Kenneth Ruud. "Benchmarking Two-Photon Absorption Cross Sections: Performance of Cc2 and Cam-B3lyp." *Physical Chemistry Chemical Physics* 17, no. 29 (2015): 19306-14.
75. Schmidt, Michael W., Kim K. Baldridge, Jerry A. Boatz, Steven T. Elbert, Mark S. Gordon, Jan H. Jensen, Shiro Koseki, Nikita Matsunaga, Kiet A. Nguyen, Shujun Su, Theresa L. Windus, Michel Dupuis, and John A. Montgomery Jr. "General Atomic and Molecular Electronic Structure System." *Journal of Computational Chemistry* 14, no. 11 (1993): 1347-63.
76. Zahariev, F., and M. S. Gordon. "Nonlinear Response Time-Dependent Density Functional Theory Combined with the Effective Fragment Potential Method." *J Chem Phys* 140, no. 18 (2014): 18A523.
77. Zaleśny, Robert, N. Arul Murugan, Guangjun Tian, Miroslav Medved', and Hans Ågren. "First-Principles Simulations of One- and Two-Photon Absorption Band Shapes of the Bis(Bf2) Core Complex." *The Journal of Physical Chemistry B* 120, no. 9 (2016): 2323-32.
78. Beerepoot, Maarten T. P., Md Mehboob Alam, Joanna Bednarska, Wojciech Bartkowiak, Kenneth Ruud, and Robert Zaleśny. "Benchmarking the Performance of Exchange-Correlation Functionals for Predicting Two-Photon Absorption Strengths." *Journal of Chemical Theory and Computation* 14, no. 7 (2018): 3677-85.
79. Choluj, M., M. M. Alam, M. T. P. Beerepoot, S. P. Sitkiewicz, E. Matito, K. Ruud, and R. Zalesny. "Choosing Bad Versus Worse: Predictions of Two-Photon-Absorption Strengths Based on Popular Density Functional Approximations." *J Chem Theory Comput* 18, no. 2 (2022): 1046-60.

80. Iozzi, M. F., B. Mennucci, J. Tomasi, and R. Cammi. "Excitation Energy Transfer (Eet) between Molecules in Condensed Matter: A Novel Application of the Polarizable Continuum Model (Pcm)." *J Chem Phys* 120, no. 15 (2004): 7029-40.
81. Blasiak, B., M. Maj, M. Cho, and R. W. Gora. "Distributed Multipolar Expansion Approach to Calculation of Excitation Energy Transfer Couplings." *J Chem Theory Comput* 11, no. 7 (2015): 3259-66.
82. Förster, Th. "Zwischenmolekulare Energiewanderung Und Fluoreszenz." *Annalen der Physik* 437, no. 1-2 (1948): 55-75.
83. Stone, A. J. "Distributed Multipole Analysis, or How to Describe a Molecular Charge Distribution." *Chemical Physics Letters* 83, no. 2 (1981): 233-39.
84. Stone, Anthony. *The Theory of Intermolecular Forces*: Oxford University Press, 2013.
85. Lu, Tian, and Feiwu Chen. "Multiwfn: A Multifunctional Wavefunction Analyzer." *Journal of Computational Chemistry* 33, no. 5 (2012): 580-92.
86. Stone, Anthony J. "Distributed Multipole Analysis: Stability for Large Basis Sets." *Journal of Chemical Theory and Computation* 1, no. 6 (2005): 1128-32.
87. Oliver, S., and C. Winter. "Metal Dithiolene Complexes for All-Optical Switching Devices." *Advanced Materials* 4, no. 2 (1992): 119-21.
88. Matsuoka, R., R. Sakamoto, T. Kambe, K. Takada, T. Kusamoto, and H. Nishihara. "Ordered Alignment of a One-Dimensional Pi-Conjugated Nickel Bis(Dithiolene) Complex Polymer Produced Via Interfacial Reactions." *Chemical Communications* 50, no. 60 (2014): 8137-39.
89. Lei Zhang, Gilles H. Peslhebre, and Heidi M. Muchall. "A General Measure of Conjugation in Biphenyls and Their Radical Cations." *Canadian Journal of Chemistry* 88, no. 11 (2010): 1175-85.
90. Serrano-Andres, L., A. Avramopoulos, J. Li, P. Labeguerie, D. Begue, V. Kello, and M. G. Papadopoulos. "Linear and Nonlinear Optical Properties of a Series of Ni-Dithiolene Derivatives." *J Chem Phys* 131, no. 13 (2009): 134312.
91. Dobrowolski, Jan Cz, and Sławomir Ostrowski. "On the Homa Index of Some Acyclic and Conducting Systems." *Rsc Advances* 5, no. 13 (2015): 9467-71.
92. Kauczor, Joanna, Patrick Norman, Ove Christiansen, and Sonia Coriani. "Communication: A Reduced-Space Algorithm for the Solution of the Complex Linear Response Equations Used in Coupled Cluster Damped Response Theory." *The Journal of Chemical Physics* 139, no. 21 (2013): 211102.
93. Thanh Phuc, Nguyen, and Akihito Ishizaki. "Control of Excitation Energy Transfer in Condensed Phase Molecular Systems by Floquet Engineering." *The Journal of Physical Chemistry Letters* 9, no. 6 (2018): 1243-48.
94. Escudero, D., and K. Veys. "Anti-Kasha Fluorescence in Molecular Entities: Central Role of Electron-Vibrational Coupling." *Accounts of Chemical Research* (2022).
95. Veys, K., and D. Escudero. "Computational Protocol to Predict Anti-Kasha Emissions: The Case of Azulene Derivatives." *Journal of Physical Chemistry A* 124, no. 36 (2020): 7228-37.
96. Escudero, D. "Revising Intramolecular Photoinduced Electron Transfer (Pet) from First-Principles." *Accounts of Chemical Research* 49, no. 9 (2016): 1816-24.
97. Rohrs, M., and D. Escudero. "Multiple Anti-Kasha Emissions in Transition-Metal Complexes." *Journal of Physical Chemistry Letters* 10, no. 19 (2019): 5798-804.